AD-A160 300 IN-FLIGHT TURBULENCE DETECTION(U) AIR FORCE GEOPHYSICS 1/1
LAB HANSCOM AFB MA A R BOHNE 08 MAR 85 AFGL-TR-85-0049

UNCLASSIFIED F/G 4/2 NL

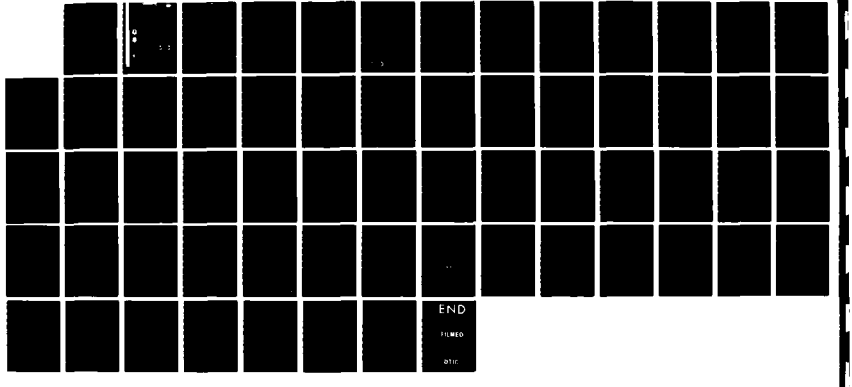

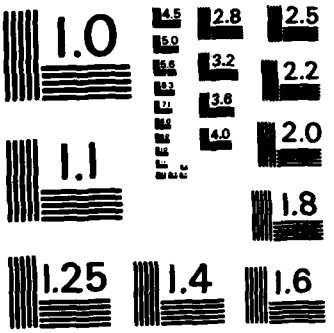

AFGL-TR-85-0049
ENVIRONMENTAL RESEARCH PAPERS, NO. 909

In-Flight Turbulence Detection

ALAN R. BOHNE

8 March 1985

ATMOSPHERIC SCIENCES DIVISION PROJECT 6670
AIR FORCE GEOPHYSICS LABORATORY
HANSCOM AFB, MA 01731

"This technical report has been reviewed and is approved for publication"

FOR THE COMMANDER

Kenneth M. Glover

KENNETH M. GLOVER
Chief, Ground Based Remote Sensing Branch
Atmospheric Sciences Division

Robert A. McClatchey

ROBERT A. MCCLATCHEY
Director, Atmospheric Sciences Division

This document has been reviewed by the ESD Public Affairs Office (PA) and is releasable to the National Technical Information Service (NTIS).

Qualified requestors may obtain additional copies from the Defense Technical Information Center. All others should apply to the National Technical Information Service.

If your address has changed, or if you wish to be removed from the mailing list, or if the addressee is no longer employed by your organization, please notify AFGL/DAA, Hanscom AFB, MA 01731. This will assist us in maintaining a current mailing list.

Unclassified

SECURITY CLASSIFICATION OF THIS PAGE

REPORT DOCUMENTATION PAGE

1a. REPORT SECURITY CLASSIFICATION: Unclassified	1b. RESTRICTIVE MARKINGS
2a. SECURITY CLASSIFICATION AUTHORITY	3. DISTRIBUTION/AVAILABILITY OF REPORT: Approved for public release; distribution unlimited.
2b. DECLASSIFICATION/DOWNGRADING SCHEDULE	
4. PERFORMING ORGANIZATION REPORT NUMBER(S): AFGL-TR-85-0049 ERP, No. 909	5. MONITORING ORGANIZATION REPORT NUMBER(S)
6a. NAME OF PERFORMING ORGANIZATION: Air Force Geophysics Laboratory; 6b. OFFICE SYMBOL (If applicable): LYR	7a. NAME OF MONITORING ORGANIZATION
6c. ADDRESS (City, State and ZIP Code): Hanscom AFB Massachusetts 01731	7b. ADDRESS (City, State and ZIP Code)
8a. NAME OF FUNDING/SPONSORING ORGANIZATION; 8b. OFFICE SYMBOL (If applicable)	9. PROCUREMENT INSTRUMENT IDENTIFICATION NUMBER
8c. ADDRESS (City, State and ZIP Code)	10. SOURCE OF FUNDING NOS.

PROGRAM ELEMENT NO.	PROJECT NO.	TASK NO.	WORK UNIT NO.
62101F	6670	15	06

11. TITLE (Include Security Classification): In-Flight Turbulence Detection

12. PERSONAL AUTHOR(S): Alan R. Bohne

13a. TYPE OF REPORT	13b. TIME COVERED	14. DATE OF REPORT (Yr., Mo., Day)	15. PAGE COUNT
Scientific—Final	FROM 10 Oct 83 TO 30 Sep 84	1985 March 8	64

16. SUPPLEMENTARY NOTATION

17. COSATI CODES			18. SUBJECT TERMS (Continue on reverse if necessary and identify by block number)
FIELD	GROUP	SUB. GR.	Incoherent radar; Turbulence severity; Doppler radar; Eddy dissipation rate; R-meter; Composite severity class

19. ABSTRACT (Continue on reverse if necessary and identify by block number)

A limited set of radar and aircraft data acquired during the 1981 and 1982 Joint Agency Turbulence Experiment are used to compare incoherent and coherent radar methods for turbulence severity estimation. Time series of ground-based radar in-phase and quadrature signal return data are processed by Doppler (Fast Fourier Transform) and incoherent (R-meter with and without noise correction) methods to determine Doppler spectrum variance. These variance data serve as input to a turbulence algorithm to derive estimates of turbulence severity. These estimates are then compared with in-situ aircraft measurements. Results show the order of preference for the radar methods is Doppler, R-meter with noise correction, and R-meter without noise correction. The R-meter without noise correction method must be considered unreliable since it results in large overestimates of turbulence severity when the signal to noise ratio is less than about 12 dB. The R-meter with noise correction method generally duplicates well the results derived from Doppler analysis and may be considered a reasonable alternative (Contd)

20. DISTRIBUTION/AVAILABILITY OF ABSTRACT	21. ABSTRACT SECURITY CLASSIFICATION
UNCLASSIFIED/UNLIMITED ☒ SAME AS RPT ☐ DTIC USERS ☐	Unclassified

22a. NAME OF RESPONSIBLE INDIVIDUAL	22b. TELEPHONE NUMBER (Include Area Code)	22c. OFFICE SYMBOL
Alan R. Bohne	(617) 861-4405	LYR

DD FORM 1473, 83 APR EDITION OF 1 JAN 73 IS OBSOLETE.

Unclassified

SECURITY CLASSIFICATION OF THIS PAGE

19. (Contd)

when Doppler capability is not available.

Preface

The data utilized in this investigation could not have been acquired without the efforts of a number of agencies and individuals. The author wishes to thank the personnel at NASA Langley Research Center and NASA Wallops Flight Center for their assistance, enabling the Air Force Geophysics Laboratory to participate effectively in the NASA Storm Hazards Program. In particular, special thanks are given to Norman Crabill, Program Manager of the Storm Hazards Program, Bruce Fisher, Project Engineer, and Jim Usry, all of NASA Langley. Robert Carr, Project Manager, and Brooks Shaw, Project Coordinator at NASA Wallops are also acknowledged. The NASA Wallops SPANDAR radar group provided crucial support in the integration of AFGL equipment into the SPANDAR radar system and continual assistance during operations. Special consideration is given to John Howard and George Bishop, Branch Managers, and Norris Beasely and Richard Gagnon, all of the SPANDAR group. AFGL was well represented, with many individuals providing crucial support in directing operations and maintaining equipment. Thanks are given to Kenneth Glober, Chief of the Ground Based Remote Sensing Branch, and Kenneth Banis, Alexander Bishop, Major Carlton Bjerkaas, Major Douglas Forsyth, Pio Petrocchi, and in particular William Smith. Special thanks are given to Graham Armstrong for designing the tracking gate recording equipment as well as participating in operations.

Contents

Illustrations

Illustrations

Tables

In-Flight Turbulence Detection

1. INTRODUCTION

The Air Force Geophysics Laboratory (AFGL) has been engaged in various efforts concerned with radar detection of turbulence in regions of precipitation. The purpose of these efforts is to develop an airborne sensor that would enable pilots to identify and avoid regions of turbulence hazardous to aircraft. Bohne[1] demonstrated the ability of ground-based radar to detect and quantify regions of hazardous turbulence. He compared estimates of turbulence severity obtained through analysis of coordinated Doppler radar data with aircraft gust data. Results showed that atmospheric turbulence could well be modeled as isotropic and as having a finite maximum turbulence scale in the range of 1 - 4 km, and that with accurate Doppler spectrum variance estimates, discrimination between hazardous and nonhazardous turbulence was possible.

This effort emphasizes application of the results and methodology developed in the previous work to data obtained from incoherent airborne radar. This investigation is important because airborne radar systems generally exhibit different characteristics from the ground-based radar utilized in the previous investigation. Examples of areas of concern would be use of the incoherent R-meter method for

(Received for publication 8 March 1985)

1. Bohne, A. R. (1985) Joint Agency Turbulence Experiment - Final Report, AFGL-TR-85-0012.

Doppler spectrum variance estimation, the relatively large beamwidth, high scan rates, moving radar platform, and stability of the airborne system. Such differences may require modification of the methods developed from the previous effort. The airborne radar data for this analysis were not available, however. Since the crucial element in reliable detection of turbulence is accurate measurement of Doppler spectrum variance, it was nonetheless considered relevant to investigate the performance of the R-meter method in detection of hazardous turbulence. Therefore, turbulence severity estimates derived from the ground-based radar data through use of both Doppler and incoherent processing methods were compared with in-situ aircraft measurements. The radar and aircraft data analyzed here were obtained from the Joint Agency Turbulence Experiment field program, where highly coordinated aircraft gust data and radar time series return data were acquired during aircraft penetrations of storms.

Estimates of Doppler spectrum variance from the various methods serve as input data to the turbulence severity estimation method suggested by Bohne,[1,2] which employs a model of the atmospheric turbulence field. Estimates of turbulence severity along the storm penetration tracks are compared to the "ground truth" severity estimates derived from the aircraft gust data.

2. COMPARISON OF RADAR SPECTRUM VARIANCE ESTIMATORS

Three methods are used to obtain the Doppler spectrum variance data used as input to the turbulence algorithm. These three methods employ: analysis of the Doppler spectrum (Hilderbrand and Sekhon[3]) and two signal amplitude level crossing rate (R-meter) methods.

The Doppler analysis uses objective thresholding of the Doppler spectra obtained from Fast Fourier analysis of the time series of in-phase and quadrature return signal data.

The crossing rate method for estimating the variance content of fluctuating Rayleigh signals was first reported by Rice[4] and later applied to meteorological phenomena by Rutkowski and Fleisher.[5] The technique was considered a reasonable approach for estimating Doppler spectrum variance when the actual Doppler spectrum was unimodal, symmetrical, and had low noise content. However, at low signal-to-noise ratios (SNR) the technique was inadequate because the uncorrelated noise signal dominated, causing overestimates of the crossing rate. Lob[6] later defined a method for correcting for low SNR and signal digitization effects.

Due to the large number of references cited above, they will not be listed here. See References, page 25.

The advent of coherent radar systems for meteorological analysis lessened the importance of the incoherent method. More recently, however, the demonstration that Doppler radar methods can detect storm regions containing hazardous turbulence has made turbulence detection a desirable feature even for incoherent radar systems.

To calculate the rate at which the signal amplitude crosses over a threshold value, the incoherent (R-meter) method uses the mean signal intensity as the threshold. Use of other threshold values was not considered, since previous investigations indicated that actual performance of the R-meter method was generally insensitive to slight modifications to the threshold value.

To recover the return signal amplitude, the magnitude of the vector formed from the two orthogonal components (the in-phase and quadrature terms) is obtained. This is done for each return signal and results in a time series of return signal amplitude.

The radar pulse repetition frequency (PRF) was 640/sec and the sample data sets contain 128 contiguous values of return data. The time series of amplitude data are used to determine the mean signal intensity for the input data sample set, and thus the signal amplitude threshold crossing level. The number of crossings through this level in the positive sense (increasing amplitude) over the sampling interval determine the threshold rate of crossing. Following Rutkowski and Fleisher, the mean signal intensity for the Rayleigh distributed return signal amplitude is

$$\langle A \rangle = 0.5\sqrt{\pi I_o}\,, \tag{1}$$

where I_o is the mean signal intensity for the sample data set and $\langle A \rangle$ is the corresponding mean intensity signal amplitude. The crossing rate W and Doppler spectrum variance VAR are related by

$$VAR = Con(W^2) \tag{2}$$

where the constant has the value

$$Con = (\lambda^2 e^{\pi/2}) / 4\pi^2 \tag{3}$$

and is (0.001359) for the radar wavelength of 10.56 cm and sample time of.20 sec used here. This relation thus returns the desired estimate of Doppler spectrum variance. Use of Eq. (2) assumes that the noise contribution to the signal amplitude is small enough so that the rate of crossing truly reflects the fluctuation of the meteorological signal.

Low SNR and signal digitization effects are corrected by putting the results of Lob into a lookup table that gives a corrected Doppler spectrum variance estimate when the threshold crossing rate and SNR are specified.

In this manner, time series of estimates of Doppler spectrum variance returned from the Doppler, standard R-meter, and Lob corrected R-meter methods are obtained.

The basic data sets used here consist of single penetration periods from each analysis day from the 1981 and 1982 seasons. Data from each day were included to keep any bias effects due to data from one day to a minimum. The time histories of Doppler spectrum variance are displayed in Appendix A and Figures 1 and 2. The time histories of penetrations on 28 and 31 July 1982 will illustrate the relative behavior of the three variance estimators.

2.1 Data From 28 July 1982

As shown in Figure 1d, the first penetration represents a period during which the SNR remains relatively constant in the range 10-12 dB, except for a few minor excursions down to about 7 dB. The variance estimates from the Doppler method (Figure 1a) show distinct periods of large spectrum variance in the range of 5-15 m^2/sec^2 with a low background value near 0.5 m^2/sec^2. The incoherent R-meter method with noise correction (Figure 1b) and without noise correction (Figure 1c) both follow well the overall pattern observed from the Doppler analysis, with periods of enhanced variance reasonably well correlated in time and magnitude with the Doppler results. The spectrum variance estimates from both incoherent methods are quite noisy, that is, rapid, easily discernible fluctuations occur throughout the time history. For the noise corrected method, this is partially a result of the finite size of the correction table employed. Background variance levels for the incoherent methods are significantly larger than for the Doppler analysis, being roughly 2 and 4 m^2/sec^2 for the Lob and standard methods, respectively. Although these large background values are minor in comparison to the magnitudes of the dominant variance peaks, such levels, particularly when the standard method is used on regions of precipitation at close range, could improperly flag storm regions as containing moderate to severe turbulence when the turbulence was actually light.

The most significant feature to consider is the behavior of the estimators during periods of reduced SNR. Periods of specific concern are 22:48:12, 22:49:01, 22:49:43 - 22:49:52, 22:50:30, 22:50:38, 22:51:09, and 22:51:22 GMT. Observation of the results from the Doppler analysis suggests only one period where noise may have influenced this estimator, that at 22:51:09 GMT. However, observation of results from Doppler analysis at even lower SNR levels (to be discussed later) suggest that the variance maximum observed here is probably a true feature. These data show that the Doppler results are essentially unaffected by low SNR.

The noise corrected trace shows two minor episodes where reduced SNR resulted in detectably larger spectrum variance (22:49:43 and 22:49:52 GMT). In contrast, the uncorrected trace shows significantly heightened variance at each reduced SNR period. The Lob R-meter method generally replicates the Doppler results well during periods of large spectrum variance, but at SNRs below 15 dB still overestimates the spectrum variance during periods when the true variance level is small. The standard R-meter method significantly overestimated the background variance value. Both incoherent methods occasionally produced periods of false large spectrum variance. Such behavior is noted at 22:49:16 and 22:49:26 GMT where large spectrum variance values are not correlated with periods of low SNR or large variance obtained through Doppler analysis.

2.2 Data From 31 July 1982

The second period for examination is presented in Figures 2a-2d for a penetration on 31 July 1982. In this example the stability of the Doppler spectrum objective thresholding method is again demonstrated by the behavior of the variance estimates at periods of very low SNR. The relative behavior of the spectrum variance histories demonstrate effects of low SNR on the crossing rate methods similar to those discussed earlier. The noise-corrected estimates of spectrum variance generally agree with those from the Doppler analysis. Once again, however, a region of false heightened spectrum variance is noted from 20:01:10 to 20:01:26 GMT. This errant behavior is even more pronounced in the results from the standard R-meter method. During all periods of low SNR, 20:01:11 - 20:01:26, 20:01:47 - 20:01:57, 20:02:26 - 20:02:33, and 20:02:54 GMT, the uncorrected method consistently returned false large variance. During periods of relatively large SNR (> 12 dB) the standard method, while in general agreement with the Doppler results, still consistently overestimated the spectrum variance.

The relative behavior noted in these two examples is also observed for the penetration periods presented in Appendix A. Generally, the crossing rate method, when corrected for noise contamination, returns estimates of Doppler spectrum variance that agree well with those obtained from objective analysis of the Doppler spectra. Without noise correction, the R-meter method is relatively good only when the SNR is greater than about 15 dB. Both incoherent methods occasionally falsely identified regions of large spectrum variance. Finally, the incoherent R-meter method overestimated the background spectrum variance, particularly when this parameter was truly small. While the Lob method generally does not result in a serious overestimate, the standard R-meter method overestimates the variance very significantly when the signal to noise ratio is less than 15 dB.

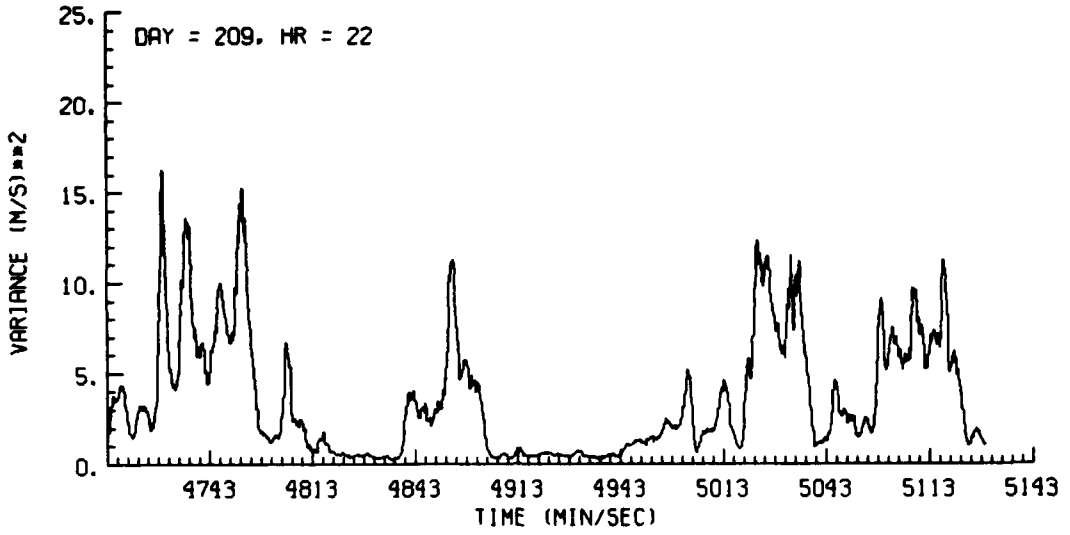

(a)

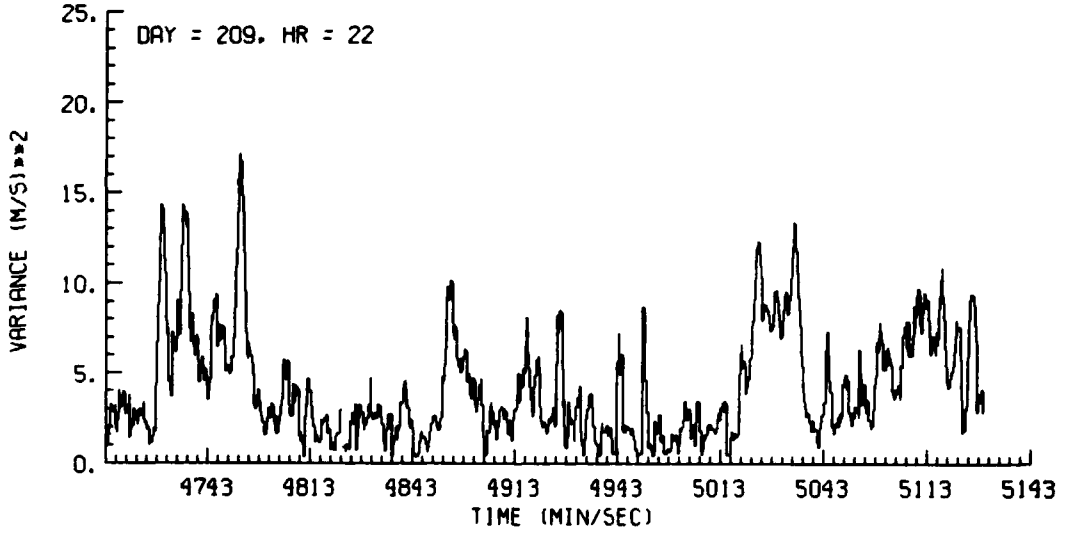

(b)

Figure 1. Time Histories of Doppler Spectrum Variance For: (a) Doppler, (b) Lob R-meter, (c) R-meter Estimators, and (d) Signal to Noise Ratio, for Penetration on 28 July 1982

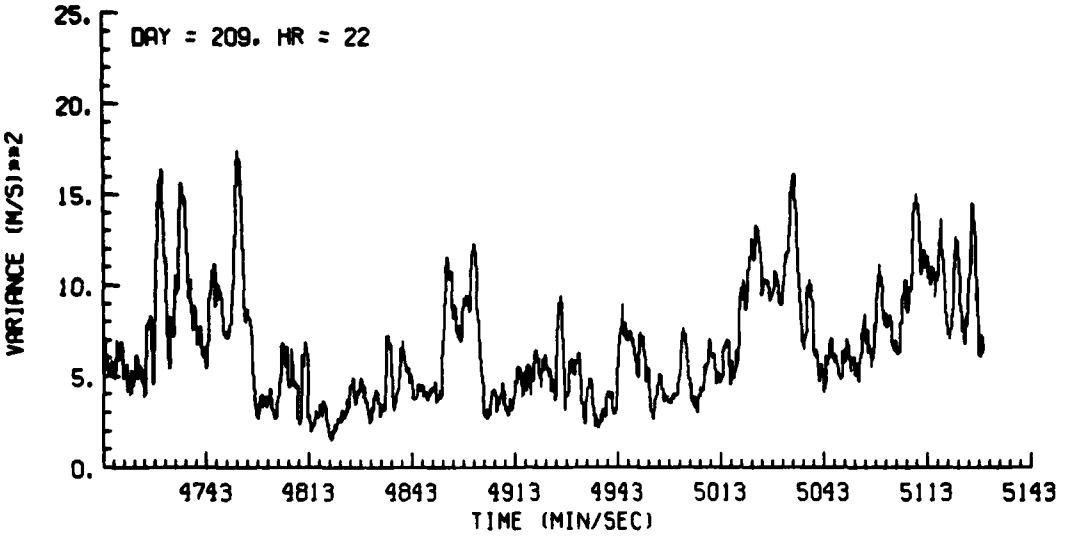

(c)

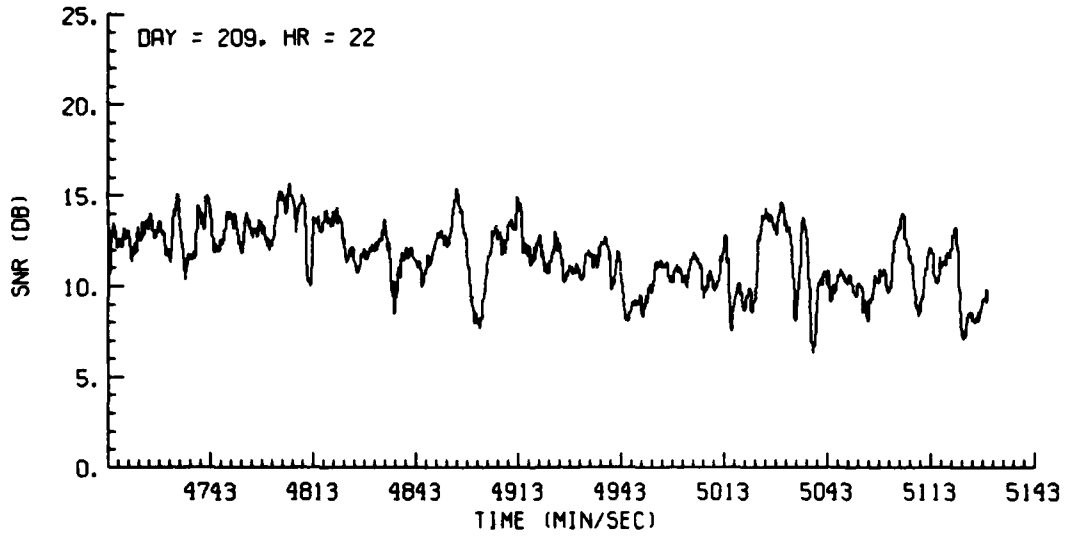

(d)

Figure 1. Time Histories of Doppler Spectrum Variance For: (a) Doppler, (b) Lob R-meter, (c) R-meter Estimators, and (d) Signal to Noise Ratio, for Penetration on 28 July 1982 (Contd)

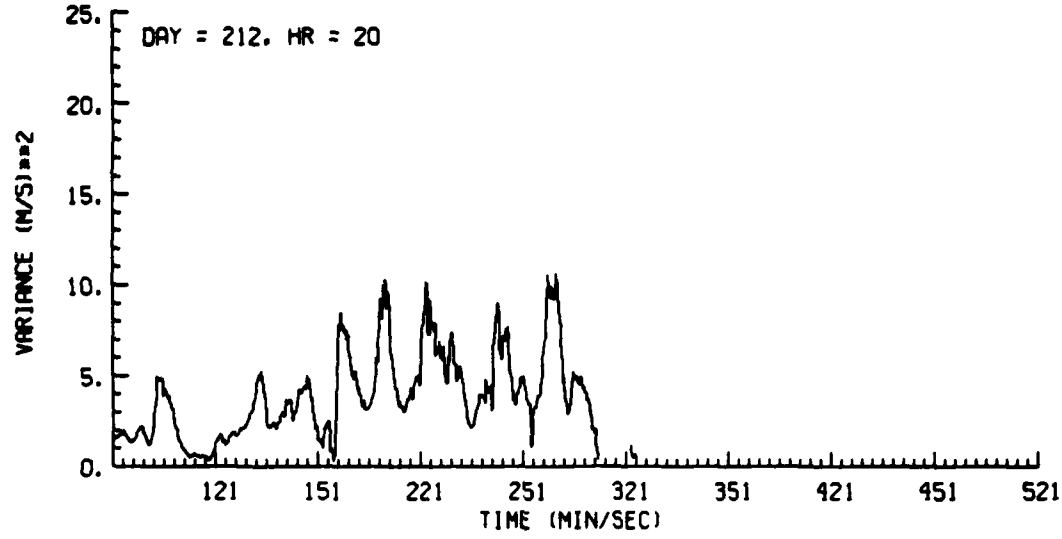

(a)

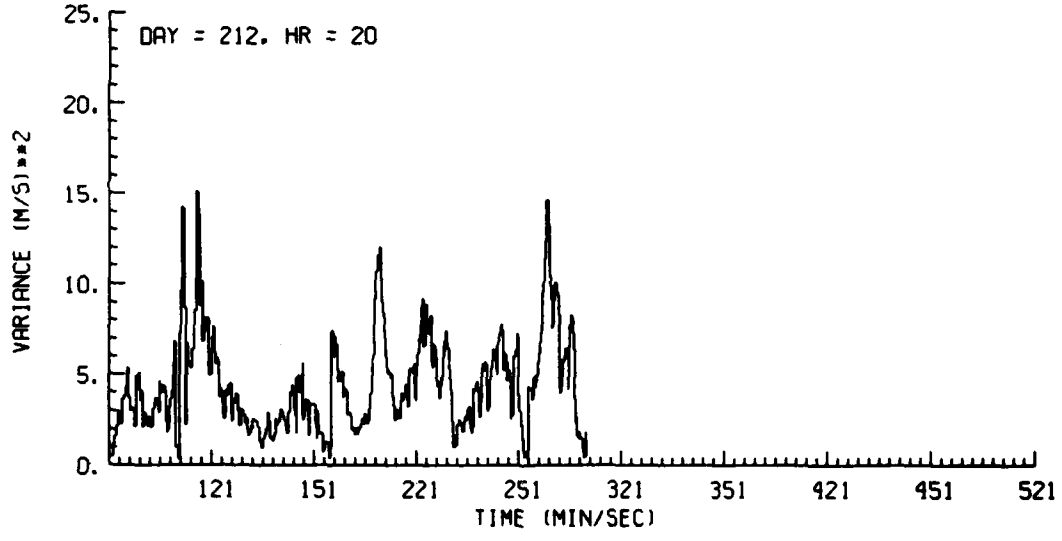

(b)

Figure 2. Time Histories of Doppler Spectrum Variance for: (a) Doppler, (b) Lob R-meter, (c) R-meter Estimators, and (d) Signal to Noise Ratio, for Penetration on 31 July 1982

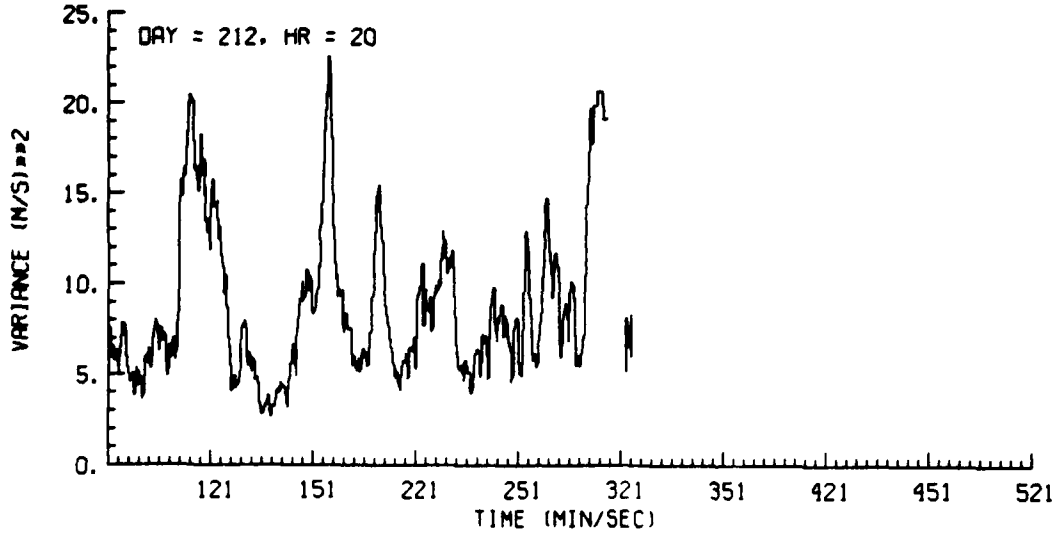

(c)

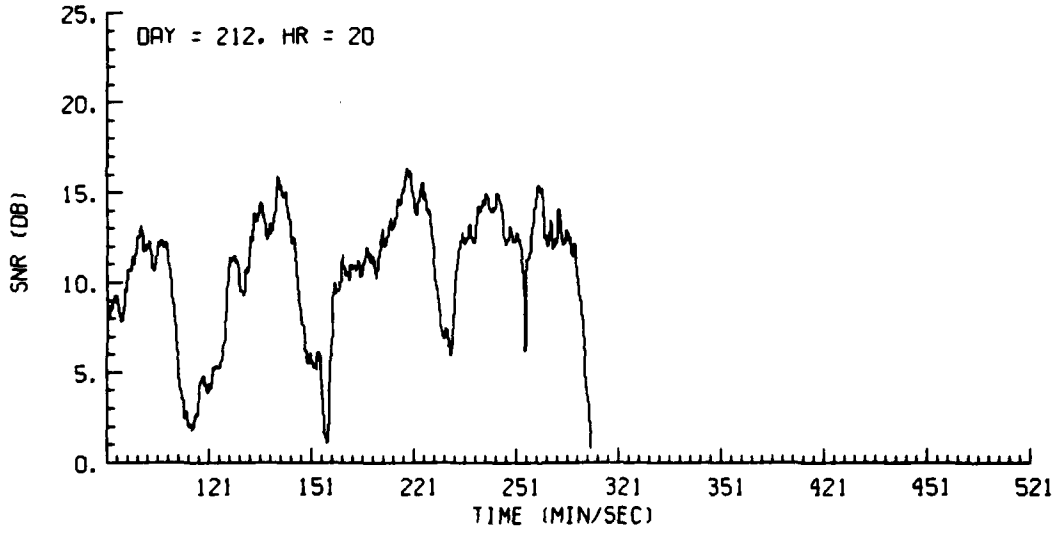

(d)

Figure 2. Time Histories of Doppler Spectrum Variance for: (a) Doppler, (b) Lob R-meter, (c) R-meter Estimators, and (d) Signal to Noise Ratio, for Penetration on 31 July 1982 (Contd)

3. COMPARISON OF RADAR AND AIRCRAFT ESTIMATES OF TURBULENCE SEVERITY

The degree of hazard of atmospheric turbulence to aircraft is determined from estimates of the turbulence severity, where turbulence severity is defined as the cube root of the eddy dissipation rate (EPS). To estimate turbulence severity, the Doppler spectrum variance data are employed in a technique discussed by Bohne,[2] which assumes that the environmental turbulence field may be modeled as inertial (Kolmogorov 5/3 law) with a finite maximum eddy size, or effective turbulence outer scale. The term effective turbulence outer scale implies that the energy contained in the environmental turbulence field, distributed over a range of scales including permanent, energy containing, and inertial subrange eddy (Kolmogorov) regimes, may be set equal to that found in the modeled field by adjustment of the turbulence outer scale. As discussed by Bohne,[1] this approach successfully models the true turbulence atmospheric environment. In the analyses presented here, an effective outer scale of 2 km was chosen for use with the radar method. This value lies in the range of preferred values, as determined from analysis of the 1981 and 1982 data.

Bohne[1] presented results indicating two major contaminants of the Doppler spectrum variance were to be expected. One of these, shear of the radial wind, could usually be neglected when estimation of turbulence severity was the only concern. Therefore, the spectrum variance data employed here are not corrected for shear contamination. However, the other contaminant, system errors, most specifically apparent channel imbalance, was corrected. The time histories of spectrum variance for the three estimators indicate the relative performance of the incoherent methods in estimating spectrum variance. However, the nonlinear relationship between Doppler spectrum variance and turbulence severity prevents determination of the relative success of the various methods in estimating turbulence severity directly from the relative performance in estimating the Doppler spectrum variance. Success or failure must be determined by comparing the capacity of the different methods to correctly assess the turbulence severity.

The applicability of the various radar techniques for estimating turbulence severity will be determined by the method used by Bohne.[1] The probability of success (POD) and false alarm rate (FAR) values for the three radar methods will be determined by comparison with the coordinated aircraft estimates of turbulence severity. Values assigned to light, moderate, heavy, and severe turbulence are those suggested by MacCready.[7] These values do not apply to all aircraft in all situations, since they depend somewhat on aircraft type and speed.

---

7. MacCready, P. (1964) Standardization of gustiness values from aircraft, J. Appl. Meteorol., 3:439-449.

Because any adjustment of the thresholds of the various turbulence severity levels would probably be upward, any technique that emphasizes the heavier turbulence regimes would probably be more successful in any new turbulence scale. As discussed in Bohne,[1] comparison over these individual severity ranges can be difficult. Therefore, comparison over the composite classification ranges suggested in Bohne[1] will be used. Two severity classes will be employed: the moderate composite class, which includes severity equal to and greater than moderate (> 1.5 cm$^{2/3}$/sec), and the heavy composite class, which includes severity equal to and greater than heavy (> 3.5 cm$^{2/3}$/sec).

The aircraft estimates of turbulence severity will serve as ground truth data against which the radar estimates will be compared. The manner in which these values are obtained is described in detail in Bohne.[1] Essentially, the aircraft data are employed in structure function analysis. The aircraft data sample set used in this analysis consisted of a 1200 m data segment centered on the location of interest. Since the aircraft speed is roughly 200 m/sec, this corresponds to about 6 sec of data. The radar data sample data sets are obtained at 0.20 sec intervals and are at a mean radar range of about 140 km. The radar beamwidth of 0.41 deg covers a length (transverse to the radar viewing direction) of about 1200 m when scanning movement is included. The radar estimates of turbulence severity are compared separately with those derived from the individual aircraft gust components. This approach is reasonable if the turbulence field is approximately isotropic, and the results should be comparable to analysis employing aircraft severity estimates determined along the radar viewing direction. Use of all three components also aids in reducing statistical, and finite sample, effects. Data analyses performed in Bohne[1] demonstrated that this approach was acceptable for these data.

The POD and FAR estimates are determined from the standard relations

$$POD = X/Z \tag{4}$$

$$FAR = Y/(X + Y) \tag{5}$$

where Z is the total number of occurrences of aircraft severity in the desired range, X is the number of simultaneous radar estimates in the same severity range, and Y is the number of radar estimates in the desired range when the aircraft value is not. Note that comparisons here are made between simultaneous aircraft and radar data. This is a stringent condition, because it assumes that the radar and aircraft data are ideally co-located. Relaxation of this condition to allow for comparison of a radar value with nearby adjacent aircraft data could also be considered a reasonable approach, and would return slightly higher POD and smaller FAR values

than those reported here. Therefore, the POD and FAR values presented here may be considered conservative.

The probability of detection and false alarm rates are presented in Table 1. For the moderate composite severity class, the three radar POD values are all near 100 percent. The associated FAR values are all 18 percent. These values are consistent with those obtained from the analysis of 35 storm penetrations of the 1981 and 1982 seasons as reported in Bohne.[1] For the heavy composite severity class, the POD values are 94, 95, and 100 percent for the Doppler, noise corrected, and uncorrected methods, respectively. The corresponding FAR values are 28, 37, and 39 percent. The success demonstrated here is somewhat better than the whole season averages reported in Bohne.[1] This is partly an artifact of the data chosen for this analysis. The penetration data utilized here generally contained a relatively high proportion of heavy turbulence severity. The data were chosen this way to ensure that sufficient data of hazardous intensity would be available for comparison. However, [when using the composite classification scheme and with the radar methods frequently overestimating turbulence severity], choosing a data set with a high proportion of strong turbulence intensity simply means that a larger proportion of the aircraft and radar severity estimates made along these penetrations will fall into the composite severity classes than was observed for the season average values reported in Bohne.[1] Observation of the behavior of the three estimators for the penetration periods discussed earlier will give a clearer picture of their performance.

Table 1. Radar Probability of Detection and False Alarm Rate
1981 and 1982 Data

Turbulence Severity ($cm^{2/3}/sec$)	Doppler		Lob R-Meter		R-Meter	
	POD	FAR	POD	FAR	POD	FAR
≥ Moderate ≥ 1.5	100	18	98	18	100	18
≥ Heavy ≥ 3.5	94	28	95	37	100	39

3.1 Turbulence Severity Estimates for 28 July

Figures 3a and 3b are the histories of turbulence severity for 28 July as obtained by use of the Doppler, LOB (solid), and standard R-meter (dash) methods. Figures 4a-4c show the corresponding turbulence severity estimates obtained from analysis of aircraft data. The peaks near 22:47:29, 22:47:35, 22:47:43, 22:47:51, 22:48:04, 22:48:43, 22:48:55, 22:50:00, 22:50:25, 22:50:33, and 22:51:05 GMT stand out in the aircraft data. The Doppler method detects these features very well, as shown in Figure 3a. The false minor peak at 22:50:12 GMT in the Doppler history is the only real failure to be observed, and is not considered significant when compared to the success in detecting the remaining severe turbulence events.

The R-meter data display mixed success. The peaks up to 22:48:54 GMT are detected by both the noise-corrected and uncorrected radar methods. Figure 1d indicates a mean SNR of about 12 dB for this time period. The two strong peaks at 22:50:24 and 22:50:34 GMT are also located quite successfully. However, during the second half of this penetration, these incoherent methods achieve only limited success as features noted in both Doppler and aircraft data (for example, 22:50:02, and 22:50:59-22:51:17 GMT) are either missing or indistinguishable from the background severity level. The consistent overestimates of severity from use of the standard R-meter method increases from the first to second half of the penetration as the mean SNR decreases from about 12 to 10 dB. Also to be noted are the peaks near 22:49:01 and 22:49:45 GMT, which are correlated with sudden reductions in the SNR at these times. Finally, from 22:49:14 to 22:49:34 GMT, both incoherent methods incorrectly detect a period of heightened turbulence severity. The values observed in this period are greater than the background level for the Lob method, but are nearly indistinguishable from the background level for the uncorrected method.

The Doppler, Lob, and standard R-meter methods all detect 100 percent of the turbulence in the moderate composite severity class. The methods have false alarm rates of 15, 15, and 16 percent, respectively. Turbulence in the heavy composite severity class is detected with a probability of 85, 94, and 100 percent, with false alarm rates of 30, 46, and 50 percent, respectively. The detection probabilities of the R-meter techniques, if taken alone, make the R-meter techniques seem more successful than the Doppler method. However, as discussed earlier, using a composite classification scheme with inflated Doppler spectrum variance, inflates the turbulence severity estimates and ultimately the POD and FAR values. The inferior performance of the standard R-meter method is shown by the fact that the increase in the FAR over the Doppler method is greater than the corresponding increase in POD.

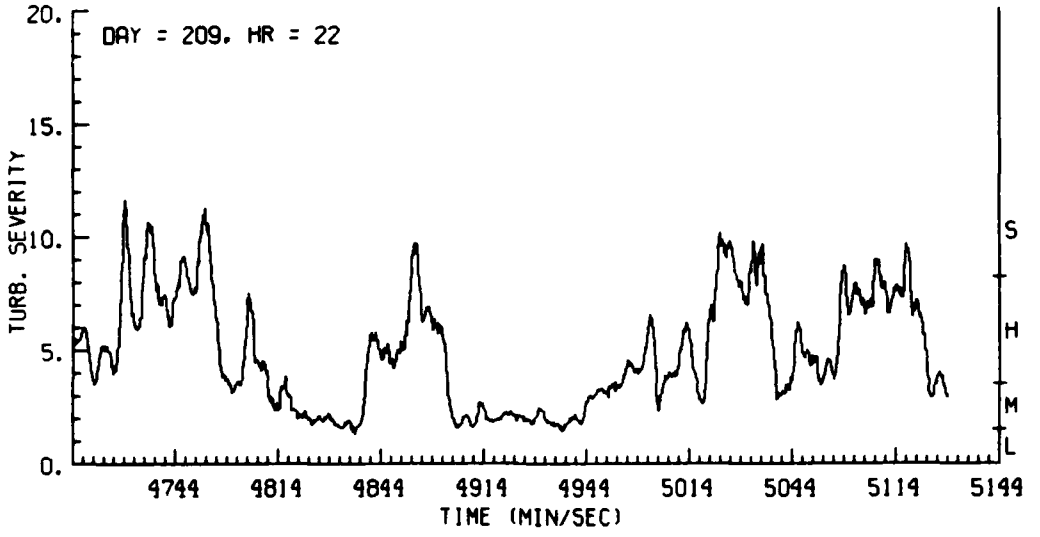

(a)

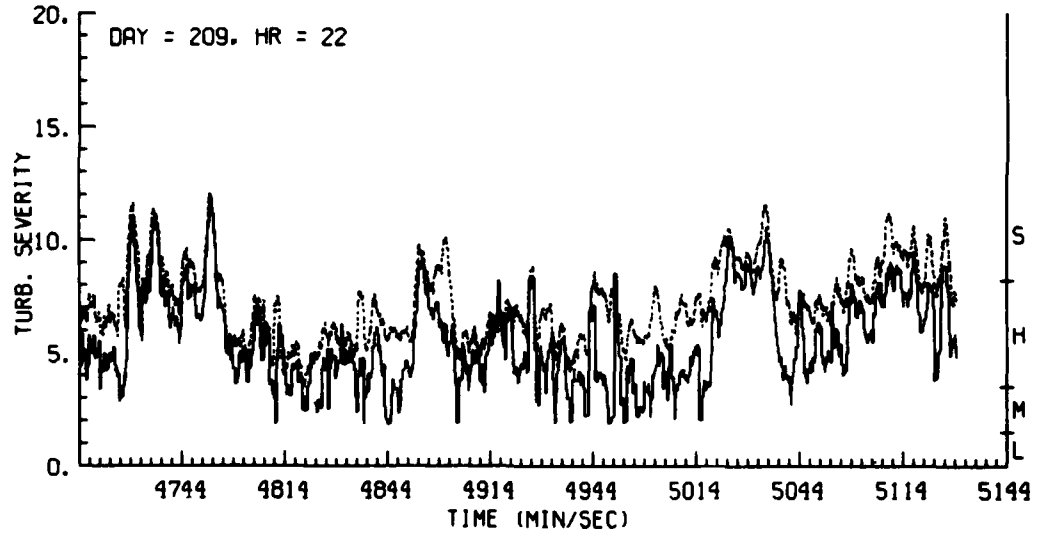

(b)

Figure 3. Time Histories of Turbulence Severity Derived From Doppler Spectrum Variance Estimates Using: (a) Doppler, and (b) Lob-R-meter and R-meter Estimators, for 28 July 1982

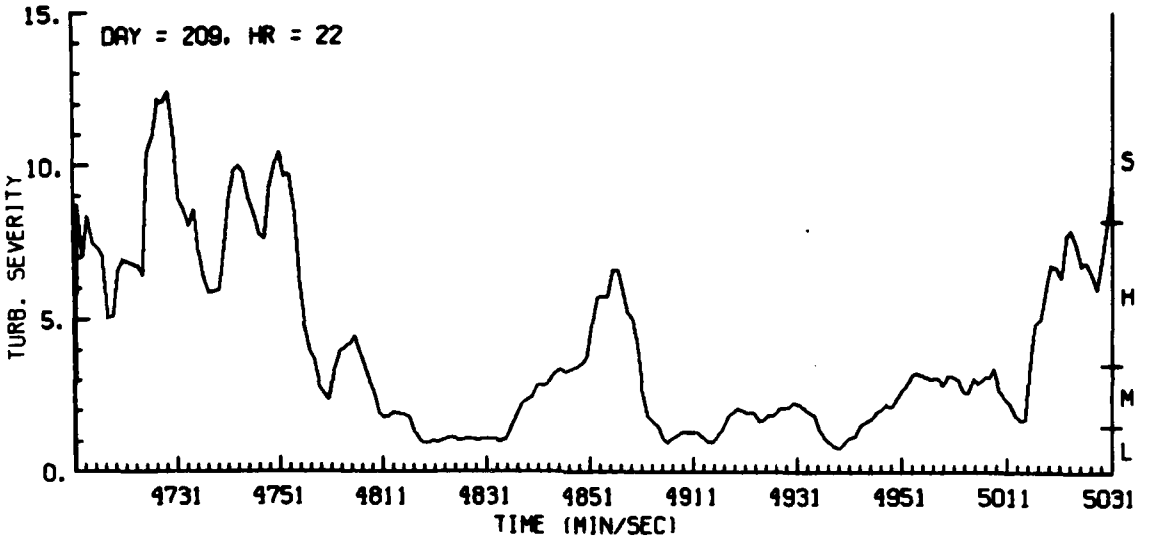

(a)

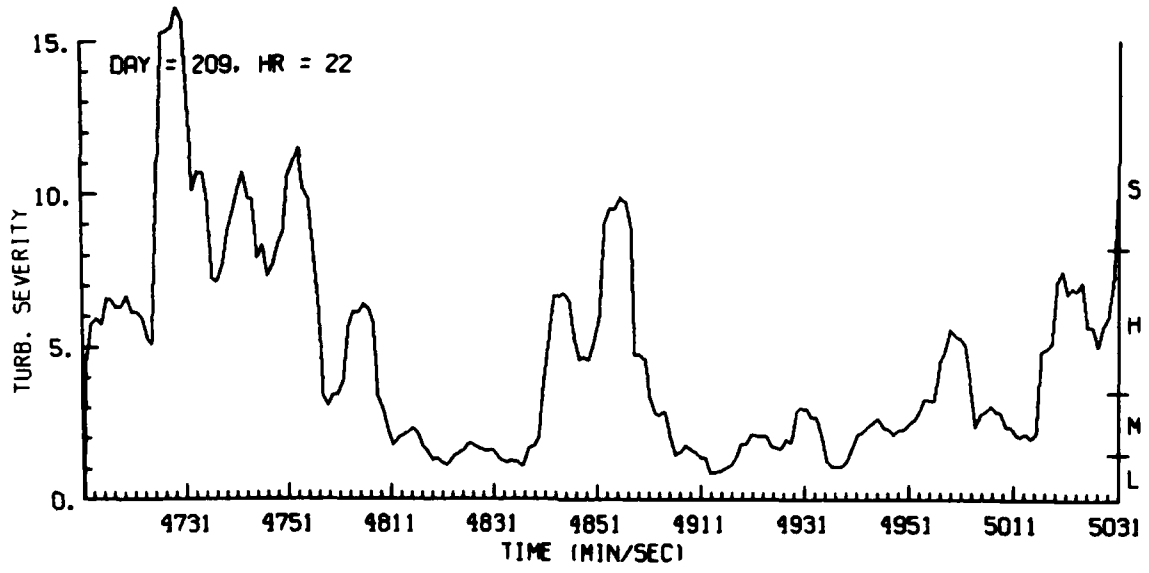

Figure 4. Time Histories of Turbulence Severity Derived From Aircraft Gust Data Along: (a) Longitudinal, (b) Lateral, and (c) Vertical Directions, for 28 July 1982

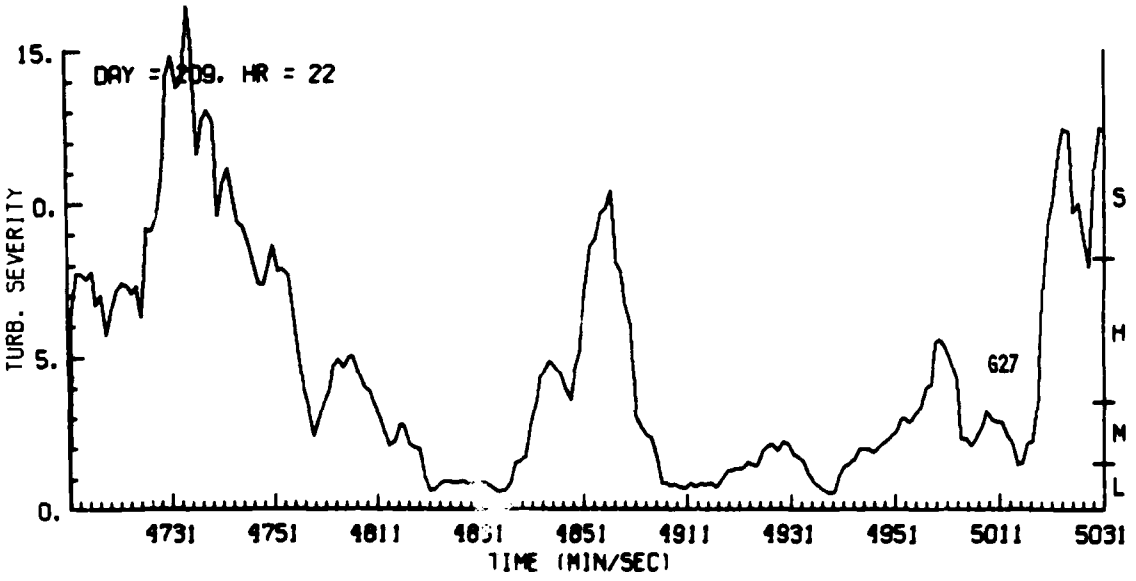

(c)

Figure 4. Time Histories of Turbulence Severity Derived From Aircraft Gust Data Along: (a) Longitudinal, (b) Lateral, and (c) Vertical Directions, for 28 July 1982 (Contd)

3.2 Turbulence Severity Estimates for 31 July

A second demonstration of the three methods is presented in Figures 5a and 5b, and 6a-6c. The significant features in the aircraft time series are the severity peaks at 20:01:01, 20:01:47, 20:01:56, 20:02:25, 20:02:46, 20:02:57, and 20:03:08 GMT, and the period of minimum severity located near 20:01:17 GMT. The severity history from the Doppler analysis shows that except for the first peak (20:01:01 GMT), all significant features are detected well. It should be noted that this first peak is essentially detected in only the lateral aircraft gust component, while the vertical gust component shows only a small corresponding peak. The Doppler-radar-observed peak centered near 20:01:06 GMT lies between this feature and a small peak detected in the aircraft data in all three gust components a short time later, at 20:01:08 GMT. This suggests that the aircraft penetrated two features, one preferentially active along the lateral aircraft gust direction, and the other uniformly distributed along all three gust directions.

Because the radar pulse volume is offset slightly from the aircraft position (typically 100-300 m), these features might have been combined in the radar pulse and observed a slightly different time at the radar offset position. A second possible

example of radar pulse volume position offset effects may be observed in the peaks observed by the aircraft near 20:02:07 and 20:02:17 GMT, which are again found primarily in the lateral and vertical gust component data, and the single radar-observed maximum near 20:02:11 GMT. The amplitudes of the peaks range from 6 to 10 $cm^{2/3}$/sec for the aircraft data and from 6 to 9 $cm^{2/3}$/sec for the Doppler radar data. The R-meter results agree with the Doppler radar and aircraft data at those locations where the SNR was about 12 dB or greater, with the incoherent methods detecting the same peaks. This was observed at 20:02:04, 20:02:45, and 20:03:00 GMT. When the SNR is close to 15 dB, the two R-meter methods produce nearly identical results.

Very different results occur when the SNR becomes low. The severity minimum located near 20:01:17 GMT in both the aircraft and Doppler severity estimates is not observed in either of the R-meter methods. Although the Lob method results are much better than those obtained from the uncorrected method, both methods incorrectly predict a period of severe turbulence. In addition, the low SNR period just before 20:01:55 GMT results in a large spike in the severity estimate made by the uncorrected R-meter method. It is apparent that the uncorrected R-meter method fails miserably during periods of low SNR and consistently overstates the severity when the SNR is less than about 12 dB. This is observed near 20:01:18, 20:01:54, 20:02:33, and 20:02:54 GMT. The Lob method duplicates the Doppler results well, and is generally reliable, but still occasionally falsely predicts periods of severe turbulence.

The POD and FAR for this penetration are very high. For the moderate composite class, the POD values are 100, 89, and 100 percent for the Doppler, corrected R-meter, and uncorrected R-meter techniques, respectively. The POD for the corrected R-meter is slightly lower than the POD for the uncorrected R-meter, because unusually low severity values were estimated during the periods of low SNR after 20:01:40 GMT. At these same times, the uncorrected R-meter had incorrectly detected strong peaks in severity. The FAR for the moderate composite class was 3 percent for all three methods. For the heavy composite severity class, the POD values are 94, 92, and 100 percent and the FAR values are 8, 11, and 11 percent, respectively. The heavy to severe aircraft turbulence that occupied most of this penetration period is not typical of the penetrations made during the 1981 and 1982 seasons. In these seasons, the turbulence severity was predominantly moderate to heavy.

The apparent success of the standard R-meter method for this penetration is an artifact of the overestimation of severity and the threshold levels chosen for moderate and heavy turbulence. This success would not be obtained in storm regions where a better mix of turbulence severity range is encountered, as was demonstrated in the previous example.

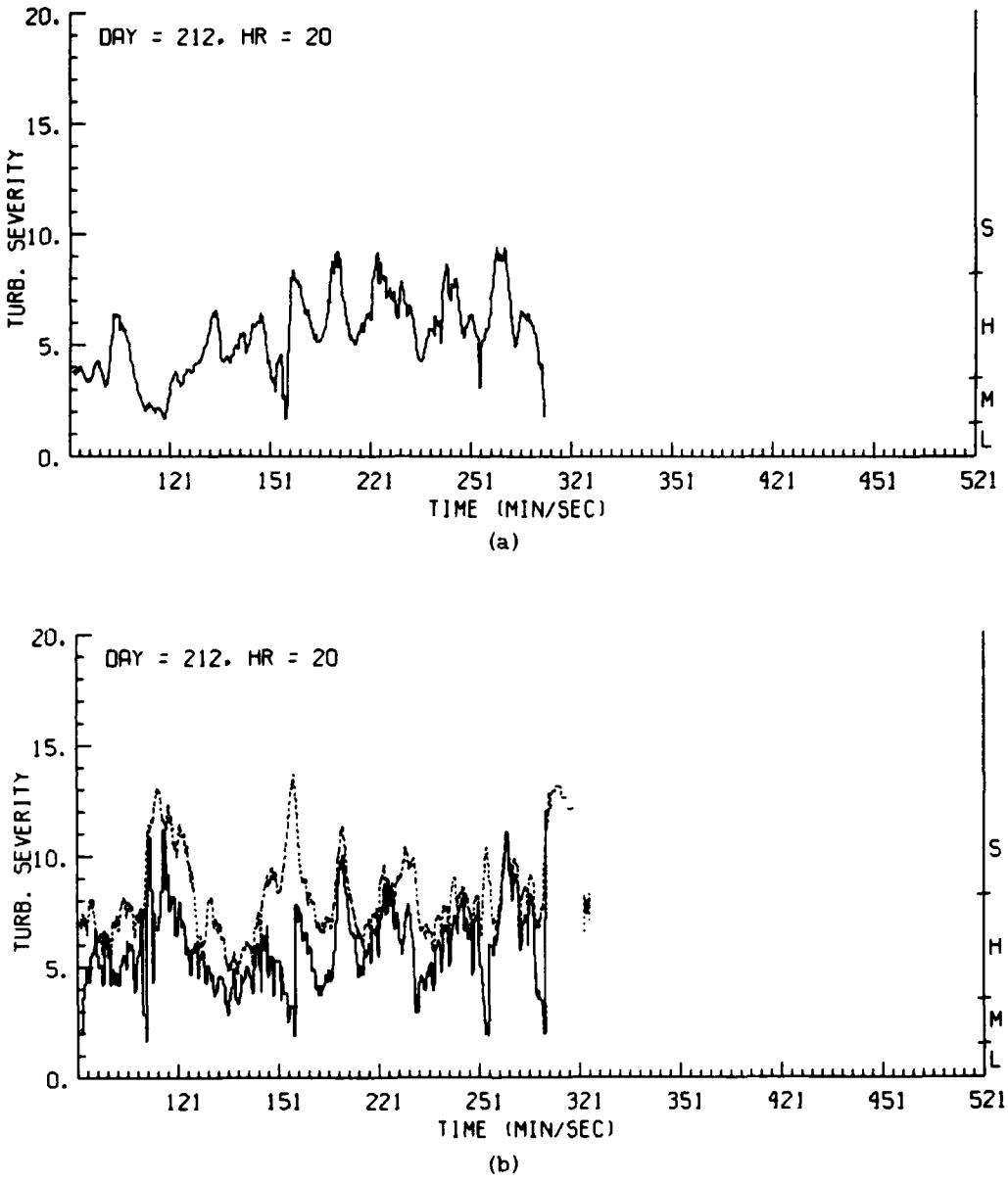

Figure 5. Time Histories of Turbulence Severity Derived From Doppler Spectrum Variance Estimates Using: (a) Doppler, and (b) Lob R-meter and R-Meter Estimators for 31 July 1982

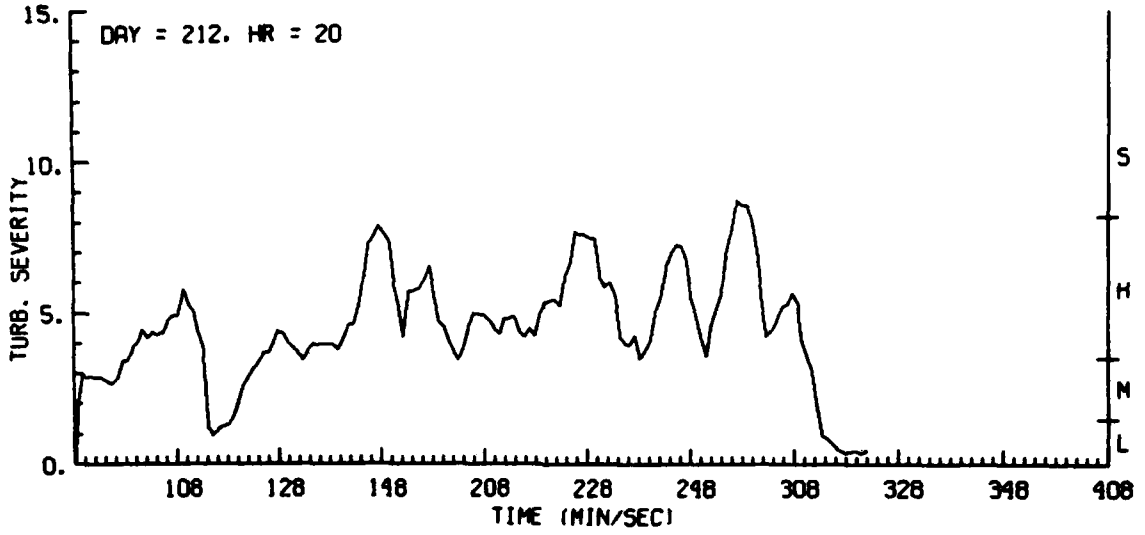

(a)

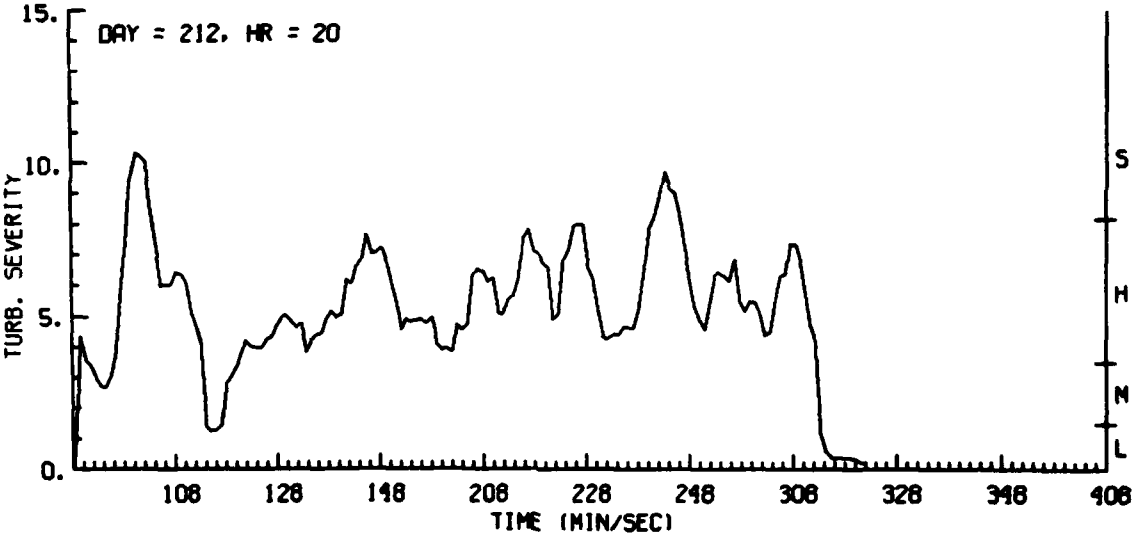

(b)

Figure 6. Time Histories of Turbulence Severity Derived From Aircraft Gust Data Along: (a) Longitudinal, (b) Lateral, and (c) Vertical Directions, for 31 July 1982

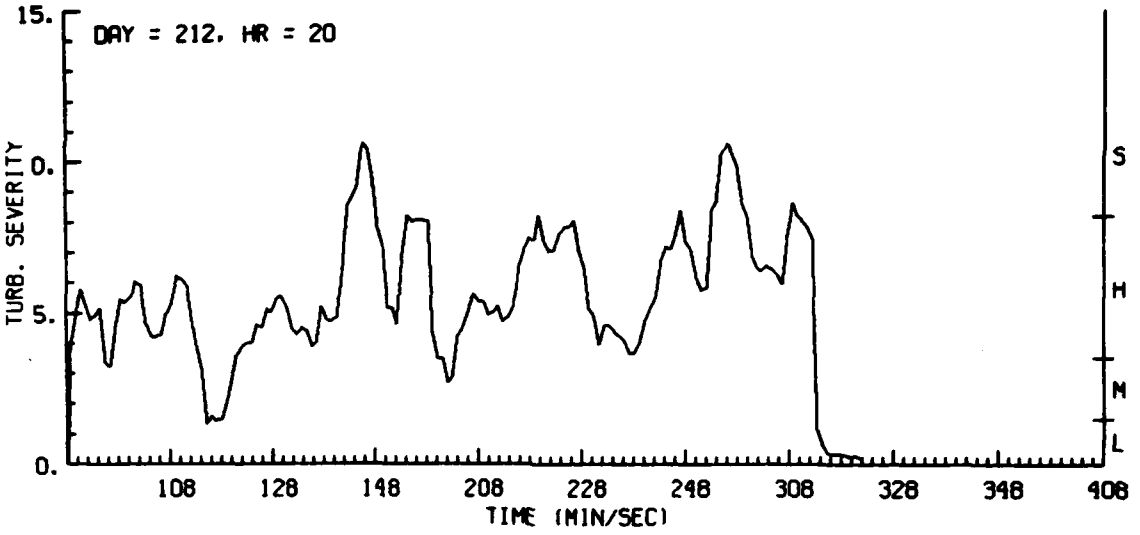

(c)

Figure 6. Time Histories of Turbulence Severity Derived From Aircraft Gust Data Along: (a) Longitudinal, (b) Lateral, and (c) Vertical Directions, for 31 July 1982 (Contd)

These time histories demonstrate that the Doppler method remains the most reliable estimator of Doppler spectrum variance for use with turbulence severity estimation methods. It has also been shown that the R-meter method with noise correction generally gives the same results as the Doppler method, whereas the R-meter method without noise correction often fails dramatically. However, it can be seen that the POD and FAR do not always properly reflect the increased accuracy of the noise-corrected R-meter technique over the uncorrected R-meter method. To clarify the interpretation of the POD and FAR results, and to further assess the relative reliability, we will modify the threshold values that designate the onset of moderate and heavy severity.

There are a number of reasons to consider the behavior of these various methods with different severity thresholds. The term turbulence severity, in the context used here, is used to describe the degree of hazard to aircraft. The indices developed by MacCready and used here were responsive more to the requirements of small aircraft than to some of the larger aircraft in use today. Any modification of the threshold levels employed here, such as for use with large aircraft, would certainly be upward. Additionally, radar estimated Doppler spectrum variance estimates are frequently artificially inflated by system noise and other effects.

The radar data employed here were carefully screened for contamination, and such effects were removed when detected. In the general case where radar system contamination is suspected one may be forced to artificially inflate the severity thresholds indicating the onset of moderate and heavy turbulence to compensate for spectrum variance overestimation. Thus, although one may employ a single method for estimation of the turbulence severity magnitude, interpretation of the degree of hazard this value represents may vary for different aircraft and radar systems. Thus, the effects on the various radar methods of varying threshold levels should be considered.

Table 3 presents the POD and FAR values for various thresholds. For the 28 July penetration one notices that as the threshold of the composite severity class increases from 2.5 to 5.5 $cm^{2/3}$/sec the POD values decrease as the range of values which represent this composite class decreases. The change is most pronounced for the Doppler and the noise corrected R-meter methods, which drop from about 95 to 75 percent. The uncorrected R-meter method retains a very high POD. The false alarm rates remain relatively constant for the Doppler and Lob R-meter methods, both increasing in magnitude by about 7 percent. However, the FAR value for the uncorrected method nearly doubles, rising from 35 to 60 percent. If 5.5 $cm^{2/3}$/sec was chosen for the threshold level for the heavy composite class, then nearly two-thirds of the storm regions flagged as containing hazardous turbulence by the standard R-meter method would be false alarms.

The goal of turbulence detection is to develop the capability to distinguish between hazardous and nonhazardous turbulent storm regions. This requires that the turbulence severity estimate be placed into the proper composite class(es), since it is whether the observation falls into both, or a single class that ultimately allows one to discriminate between hazardous and nonhazardous turbulence. As shown here, use of the standard R-meter method can result in large overestimates of the turbulence severity, often resulting in the measurement falling into both composite classes. This makes discrimination between hazardous and nonhazardous severity difficult. This difficulty is mirrored in the FAR values of the method for the two composite classes. Thus it is clear that the most appropriate approach is the method that exhibits the best combination of high POD and low FAR, and is ultimately the method that duplicates the in-situ measurements best. The POD and FAR values presented for this penetration are expected to mirror well the season averages. From these results, it is quite apparent that the order of preference is the Doppler, Lob R-meter, and last the standard R-meter method, respectively.

Table 2. Radar Probability of Detection and False Alarm Rate

Turbulence Severity ($cm^{2/3}/sec$)	Doppler		Lob R-Meter		R-Meter	
	POD	FAR	POD	FAR	POD	FAR
28 July 1982						
≥ Moderate ≥ 1.5	100	15	100	16	100	16
≥ Heavy ≥ 3.5	85	30	94	46	100	50
31 July 1982						
≥ Moderate ≥ 1.5	100	3	89	3	100	3
≥ Heavy ≥ 3.5	94	8	92	11	100	11

Table 3. Radar Probability of Detection and False Alarm Rate Variation With Threshold

Turbulence ($cm^{2/3}/sec$)	Doppler		Lob R-Meter		R-Meter	
	POD	FAR	POD	FAR	POD	FAR
28 July 1982						
≥ 2.5	90	22	96	34	100	35
≥ 3.5	85	30	94	46	100	50
≥ 4.5	77	28	82	45	99	57
≥ 5.5	71	29	74	46	94	60
31 July 1982						
≥ 2.5	97	3	96	4	100	4
≥ 3.5	94	8	92	11	100	11
≥ 4.5	87	27	81	30	100	34
≥ 5.5	71	53	70	53	99	59

The data for 31 July also show decreases in POD and corresponding increases in FAR. Although these data are considered atypical of that commonly observed in general penetrations, they do provide additional insight into the use of the composite classification scheme. Whereas there was a gradual change in the POD and FAR

values of these estimates for the previous penetration period, here two dramatic increases, detected particularly in the FAR results, are observed for threshold levels of 4.5 and 5.5 $cm^{2/3}/sec$. This results primarily from the high background severity level of 4 - 6 $cm^{2/3}/sec$ in the ground truth aircraft data. When the threshold rises through the aircraft background level, a large amount of aircraft data is removed from the composite class under consideration. With the radar methods generally overestimating the turbulence severity background level, with the overestimate ranging from small for the Doppler method to large for the standard R-meter method, a corresponding drop need not be observed in the radar data. Thus the sudden increase in FAR results from the thresholds lying just above a general aircraft severity threshold and below the corresponding radar value.

The use of composite turbulence severity levels presented in Bohne[1] was suggested as a means to discriminate between moderate and heavy, thus nonhazardous and hazardous, turbulence. This implies that all observations will be assigned to one of two classes of severity with moderate turbulence considered present when the moderate composite threshold is crossed, but the heavy composite threshold is not. For proper discrimination between nonhazardous and hazardous storm regions, the most successful method will be that which enjoys the best combination of high POD and low FAR and best duplicates the in-situ aircraft measurements. The POD and FAR values for the standard composite classes presented in Table 1 portray the general behavior to be expected by the three techniques in storm regions generally containing moderate to severe turbulence. It is clear that the Doppler method returns the best combination of POD and FAR values and easily is the method that best duplicates the in-situ aircraft results. The noise corrected method, however, also enjoys considerable success, although it occasionally overestimates the turbulence severity, causing more false alarms. The effects of higher FAR become increasingly important if one considers raising the threshold levels for the composite classes. The uncorrected R-meter method is equivalent to the Lob method when the SNR is greater than about 15 dB. Below an SNR of about 12 dB, this method begins to severely overestimate the turbulence severity and high FAR values ensue. Thus although the Doppler method is preferred, the noise corrected R-meter method suggested by Lob appears to be a reasonable substitute when Doppler capability is not available. The R-meter method without noise correction is not considered practical since large portions of storms may be expected to exhibit radar SNR values below 15 dB, where this method becomes very unreliable.

4. CONCLUSIONS

Due to unavailability of airborne radar data a complete test of the applicability of the turbulence intensity estimation technique with airborne radar systems was not possible. However, success in detecting regions of significant turbulence demands accurate estimation of Doppler spectrum variance. A limited data set, consisting of seven penetration periods acquired during the Joint Agency Turbulence Experiment, were analyzed. Coordinated aircraft gust data and ground-based radar time series data were used to estimate the turbulence severity during storm penetration periods. The radar values were compared with those from the in-situ "ground truth" aircraft estimates. The penetration periods chosen contained a high proportion of intense turbulence and are in storm regions which, without turbulence information, could normally be considered suitable for penetration by aircraft.

Estimates of turbulence severity from the radar data were obtained using a modeled turbulence field with an effective outer scale of 2 km. The signal to noise ratio levels for these penetration periods typically ranged from 2 to 18 dB. Applicability of the methods for turbulence detection was based on probability of detection and false alarm rate measurements and the ability of the radar methods to duplicate the in-situ aircraft observations. A composite turbulence severity classification scheme was utilized. The Doppler method was found to accurately duplicate the features, both in magnitude and location, observed in the aircraft data. The incoherent method with noise correction generally detects these features with only occasional failures. The reasons for failures are at present unexplained but are not correlated with low signal to noise ratio events. As expected, the incoherent method without noise correlation is unreliable during low signal power periods, consistently detecting false episodes of severe turbulence. This method should be considered unreliable when the signal to noise ratio is 12 dB or less. Use of the noise corrected R-meter method demands continuous, accurate measurements of the signal to noise ratio. Here the signal to noise ratio was determined for each individual Doppler spectrum variance estimate. Methods for estimating this parameter, such as use of a single range gate at a location containing no meteorological signal, or other noise monitoring technique which makes one noise measurement for an entire radial of data would seem reasonable only if the mean noise power remains constant over the period required to obtain the data sample set.

The results show that the incoherent method with noise correction appears to be a reasonable alternative approach for providing turbulence detection capability to radar systems which are not coherent. The results presented here do not provide a measure of the effects introduced by radar systems scanning from a moving platform. Thus a more decisive test of the approach requires analysis with actual airborne radar data.

References

1. Bohne, A. R. (1985) Joint Agency Turbulence Experiment - Final Report, AFGL-TR-85-0012.
2. Bohne, A. R. (1982) Radar detection of turbulence in precipitation environments, J. Atmos. Sci., 39:1819-1837.
3. Hildebrand, P. H., and Sekhon, R. S. (1973) Objective Determination of the Noise Level in Doppler Spectra, Tech. Report 32., Lab. Atmos. Prob., University of Chicago.
4. Rice, S. D. (1944-45) Mathematical analysis of random noise, Bell Syst. Tech. J., 23:282-232, and 24:46-156.
5. Rutkowski, W., and Fleisher, A. (1955) The R-meter an Instrument for Measuring Gustiness, MIT Wea. Radar Res. Dept., No. 24.
6. Lob, W. H. (1963) R-meter correction for boxcarring and receiver noise in incoherent weather radars, J. Appl. Meteorol., 7:1018-1025.
7. MacCready, P. (1964) Standardization of gustiness values from aircraft J. Appl. Meteorol., 3:439-449.

Appendix A

Doppler Spectrum Variance Estimates

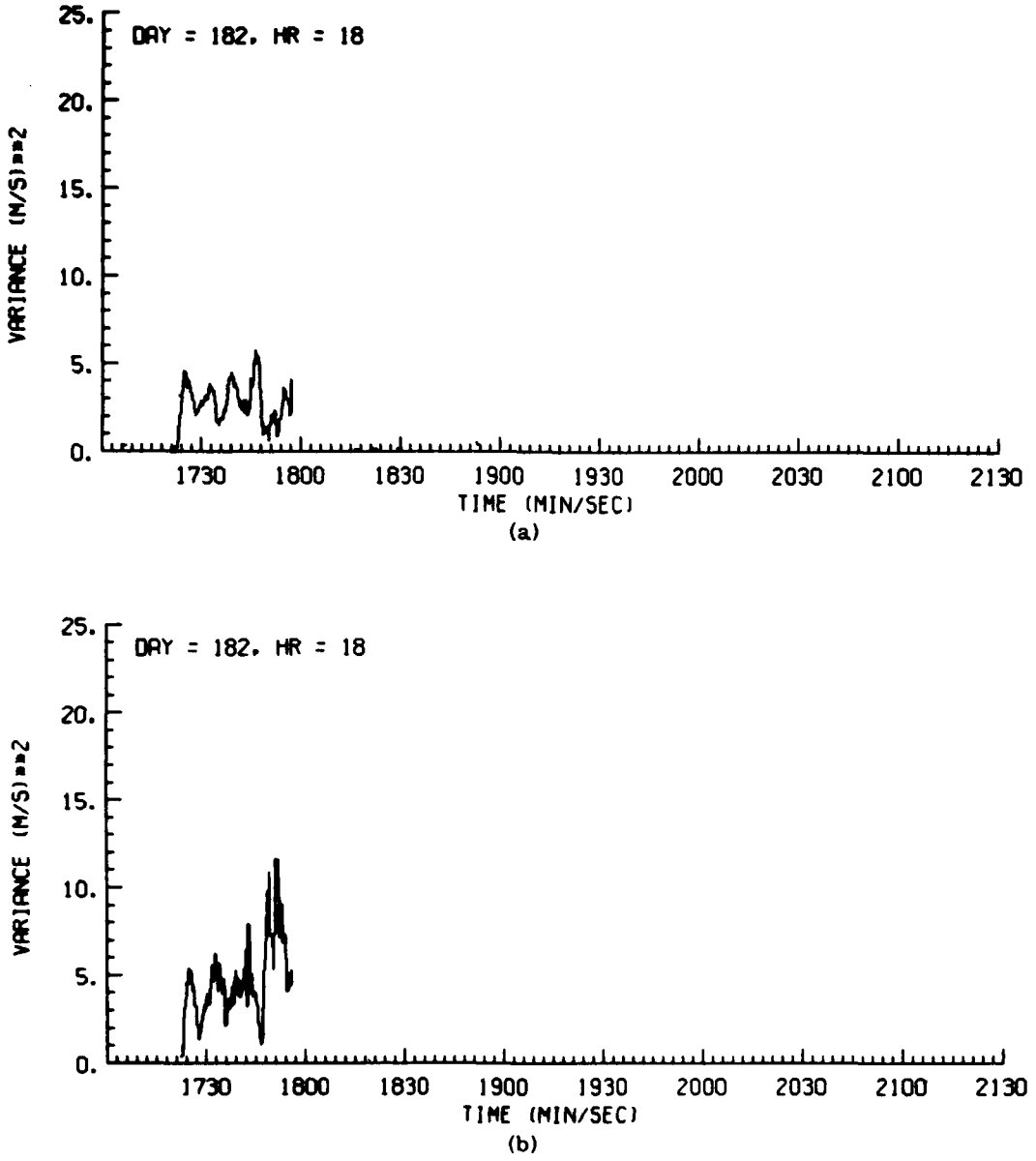

Figure A1. Time Histories of Doppler Spectrum Variance for: (a) Doppler, (b) Lob R-meter, (c) R-meter Estimators, and (d) Signal to Noise Ratio, for Penetration on 1 July 1981

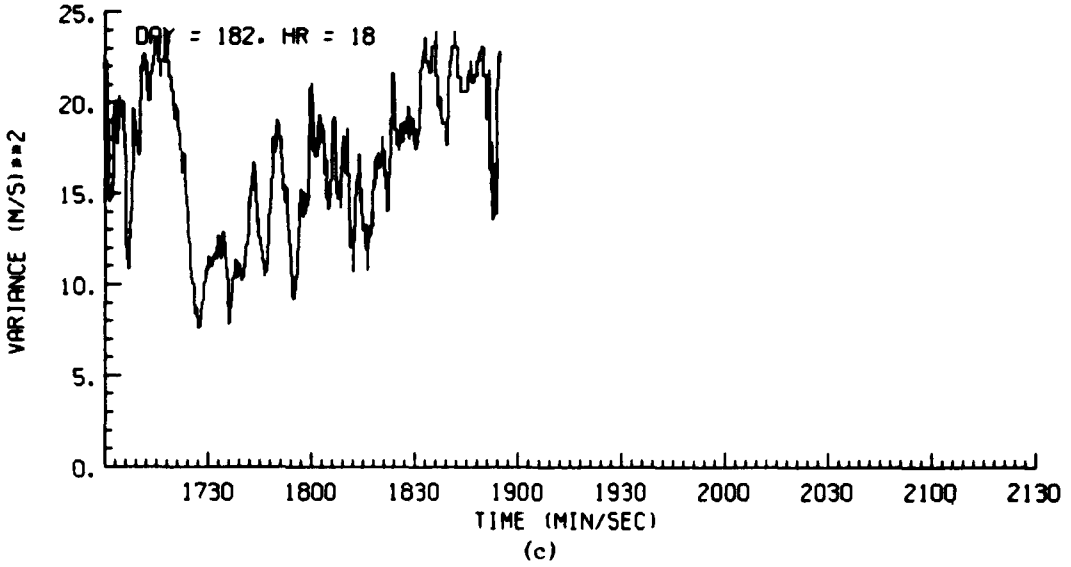

(c)

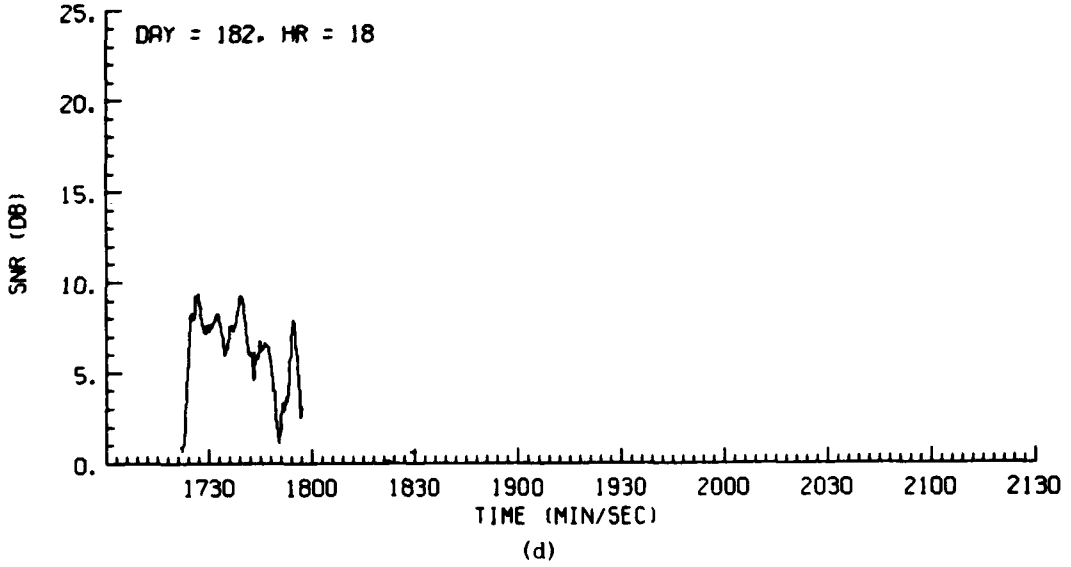

(d)

Figure A1. Time Histories of Doppler Spectrum Variance for: (a) Doppler, (b) Lob R-meter, (c) R-meter Estimators, and (d) Signal to Noise Ratio, for Penetration on 1 July 1981 (Contd)

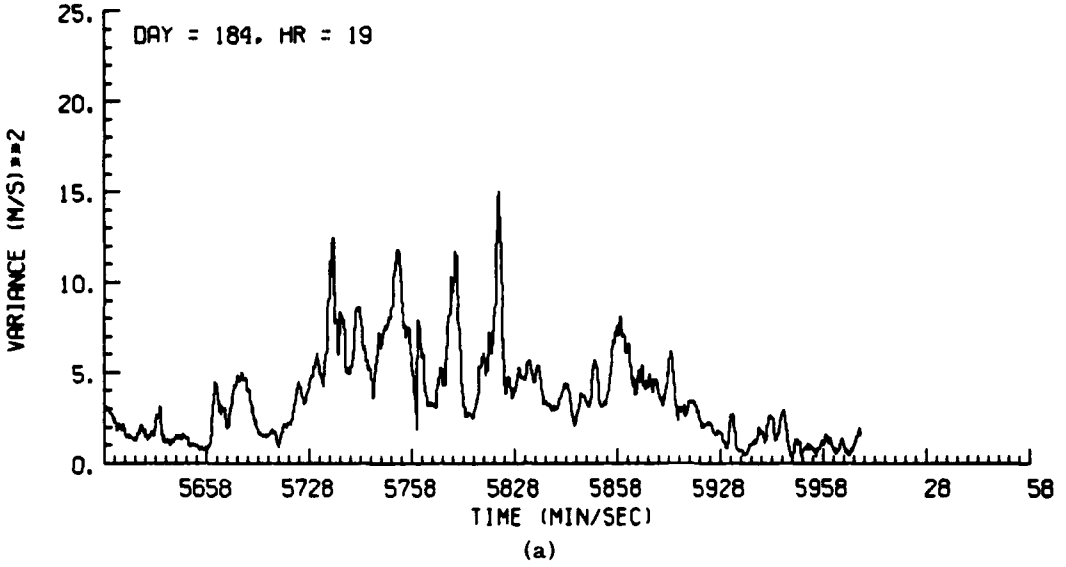

(a)

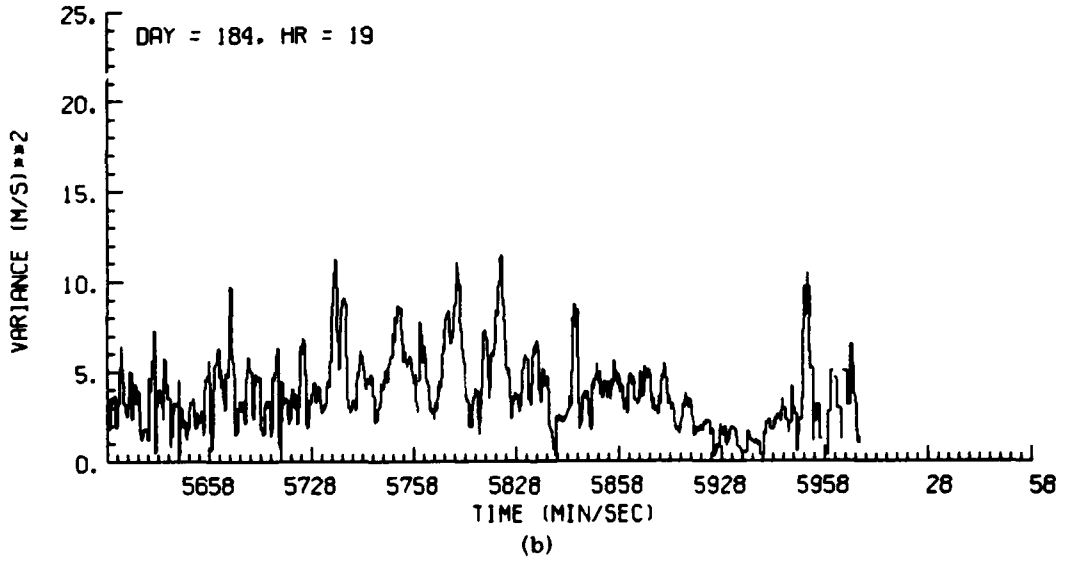

(b)

Figure A2. Time Histories of Doppler Spectrum Variance for; (a) Doppler, (b) Lob R-meter, (c) R-meter Estimators, and (d) Signal to Noise Ratio, for Penetration on 3 July 1981

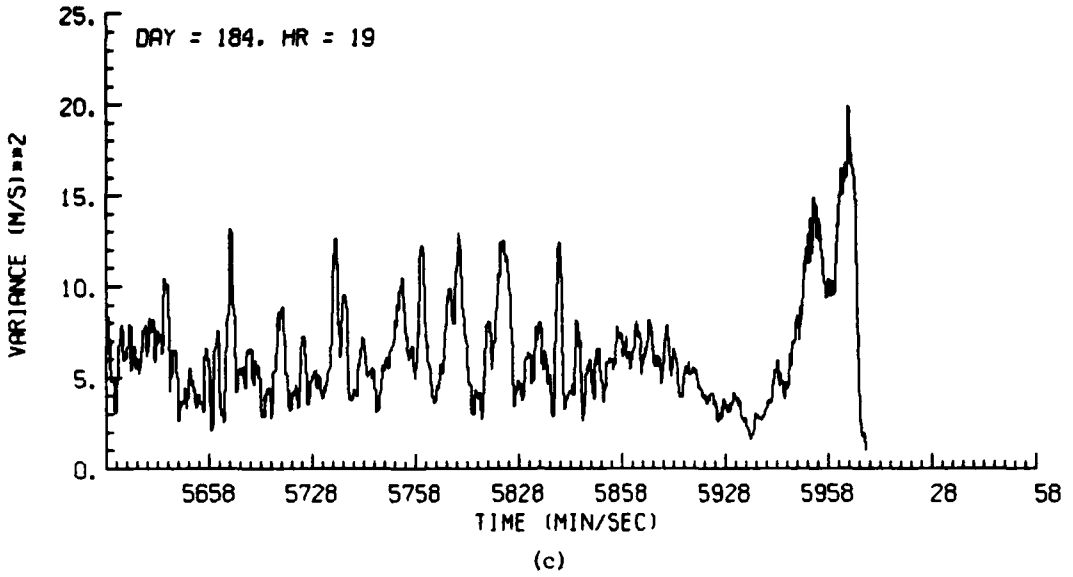

(c)

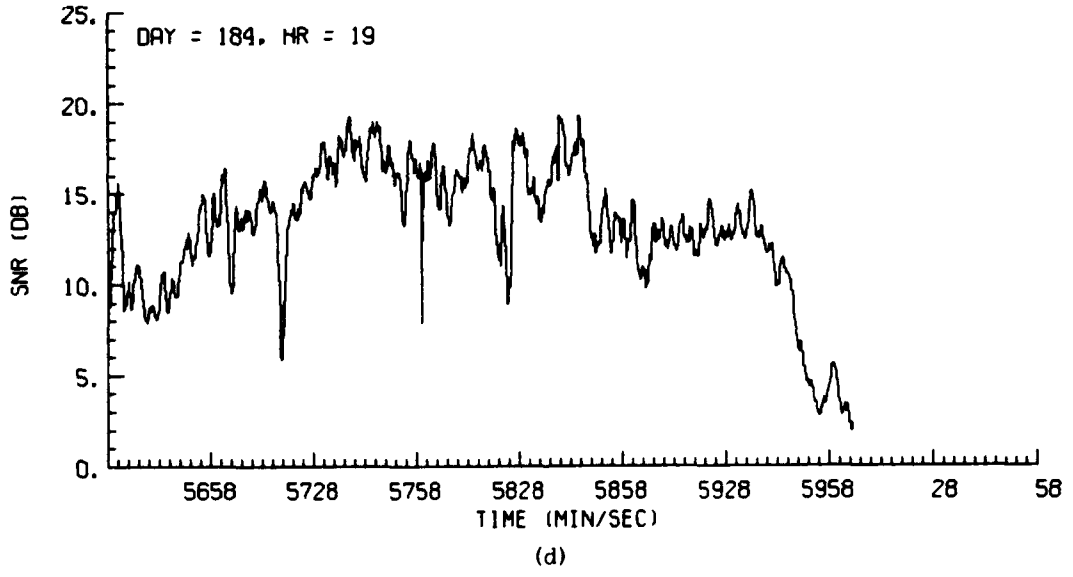

(d)

Figure A2. Time Histories of Doppler Spectrum Variance for: (a) Doppler, (b) Lob R-meter, (c) R-meter Estimators, and (d) Signal to Noise Ratio, for Penetration on 3 July 1981 (Contd)

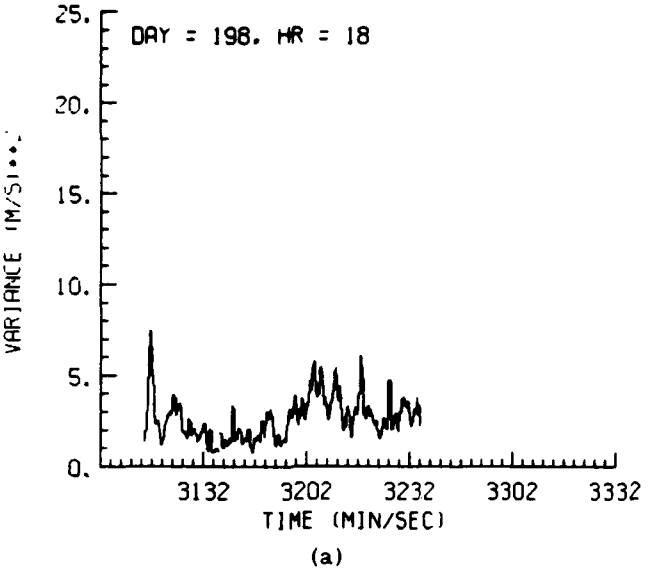

(a)

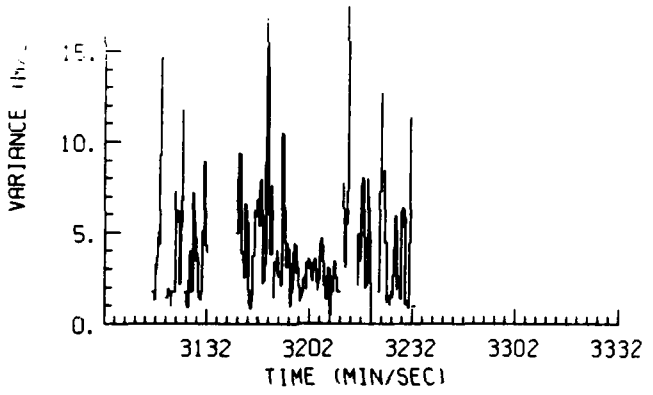

(b)

Figure A3. Time Histories of Doppler Spectrum Variance for: (a) Doppler, (b) Lob R-meter, (c) R-meter Estimators, and (d) Signal to Noise Ratio, for Penetration on 17 July 1981

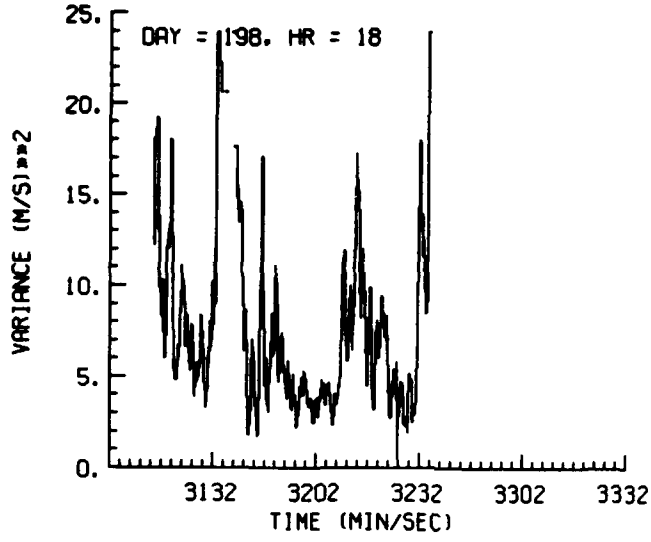

(c)

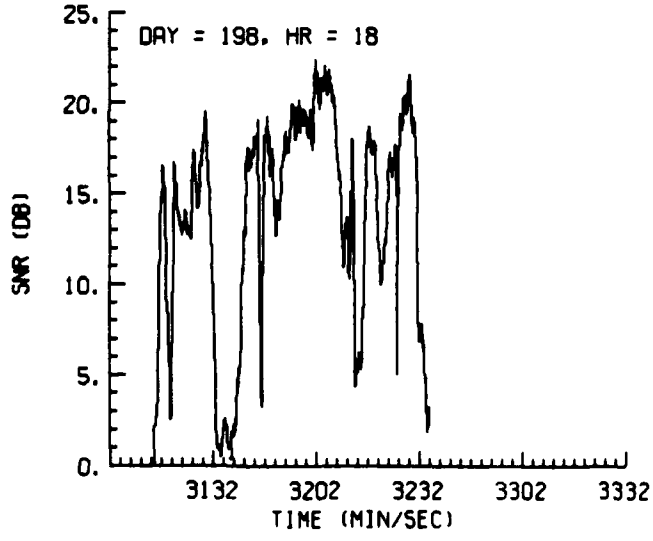

(d)

Figure A3. Time Histories of Doppler Spectrum Variance for: (a) Doppler, (b) Lob R-meter, (c) R-meter Estimators, and (d) Signal to Noise Ratio, for Penetration on 17 July 1981 (Contd)

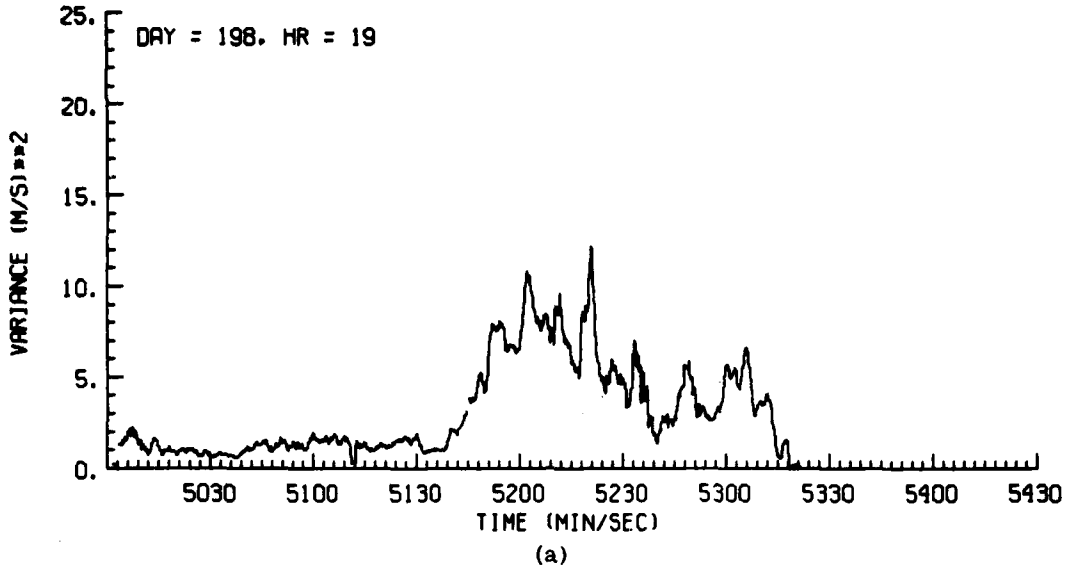

(a)

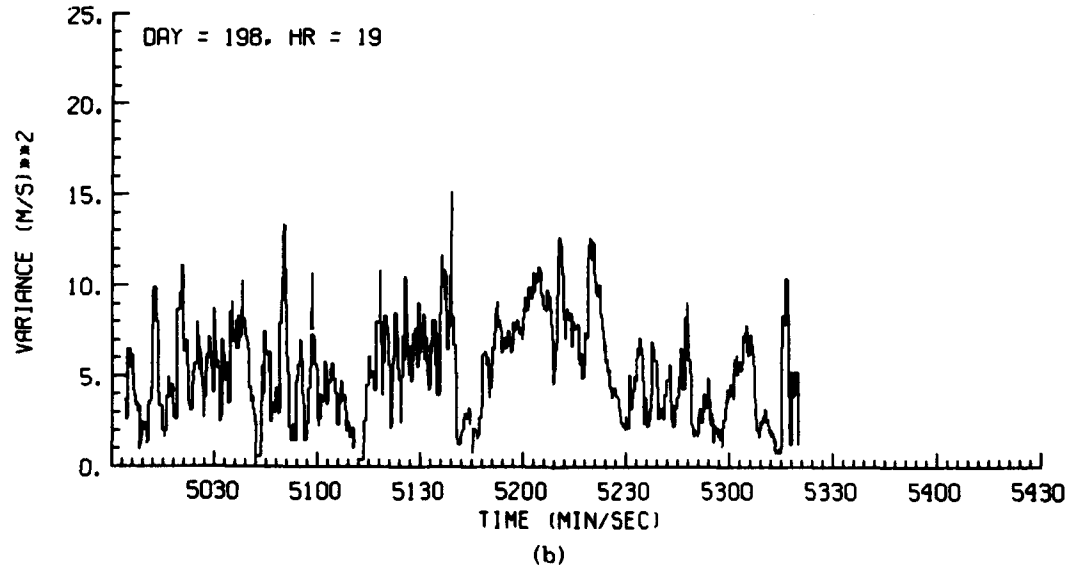

(b)

Figure A4. Time Histories of Doppler Spectrum Variance for: (a) Doppler, (b) Lob R-meter, (c) R-meter Estimators, and (d) Signal to Noise Ratio, for Penetration on 17 July 1982

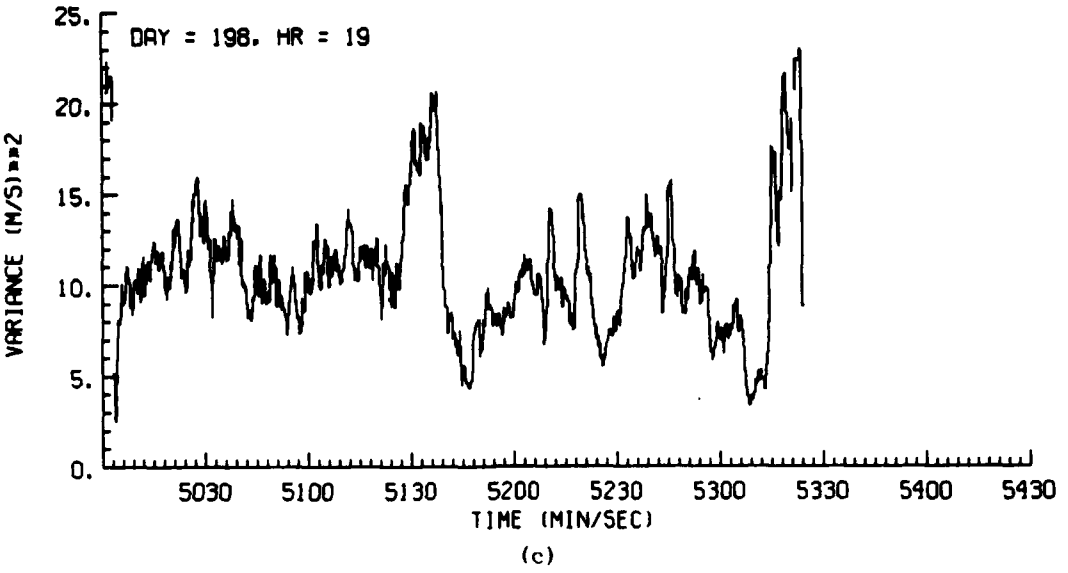

(c)

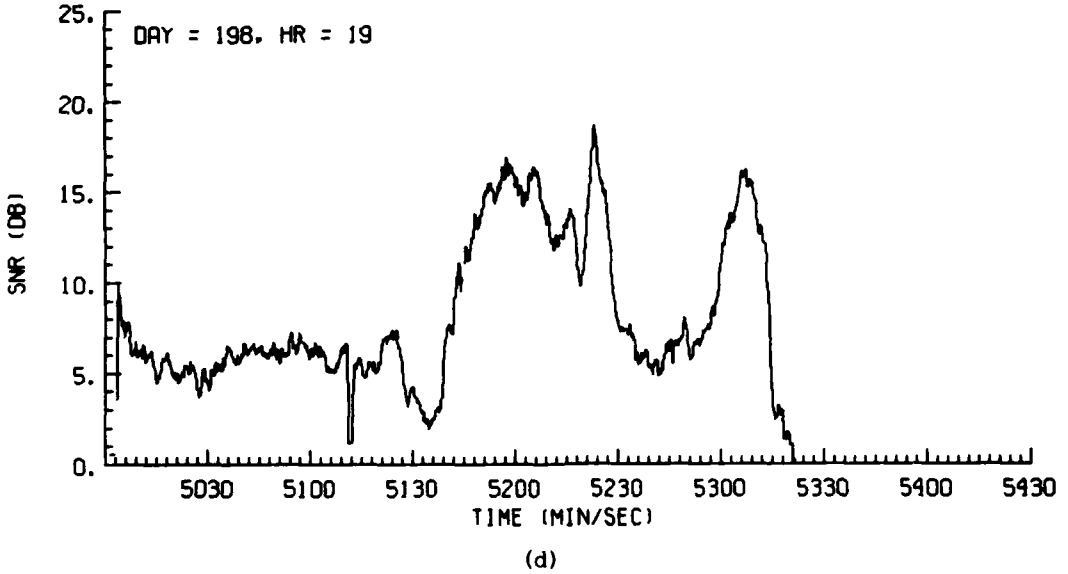

(d)

Figure A4. Time Histories of Doppler Spectrum Variance for: (a) Doppler, (b) Lob R-meter, (c) R-meter Estimators, and (d) Signal to Noise Ratio, for Penetration on 17 July 1982 (Contd)

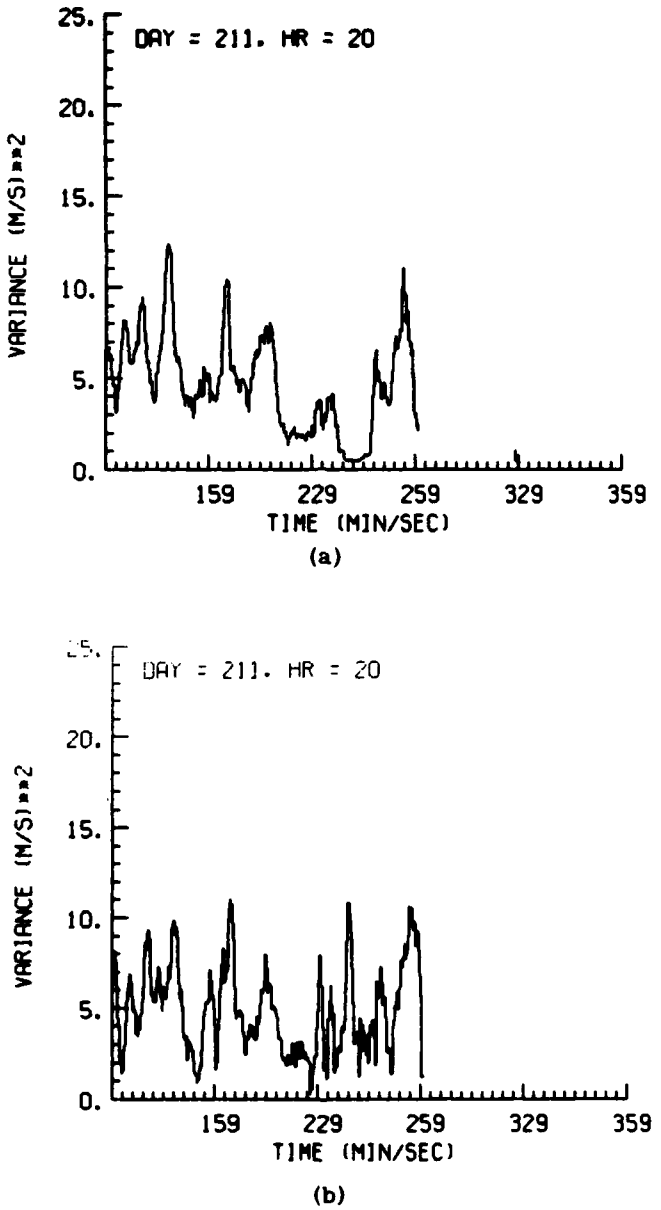

Figure A5. Time Histories of Doppler Spectrum Variance for: (a) Doppler, (b) Lob R-meter, (c) R-meter Estimators, and (d) Signal to Noise Ratio, for Penetration on 30 July 1982

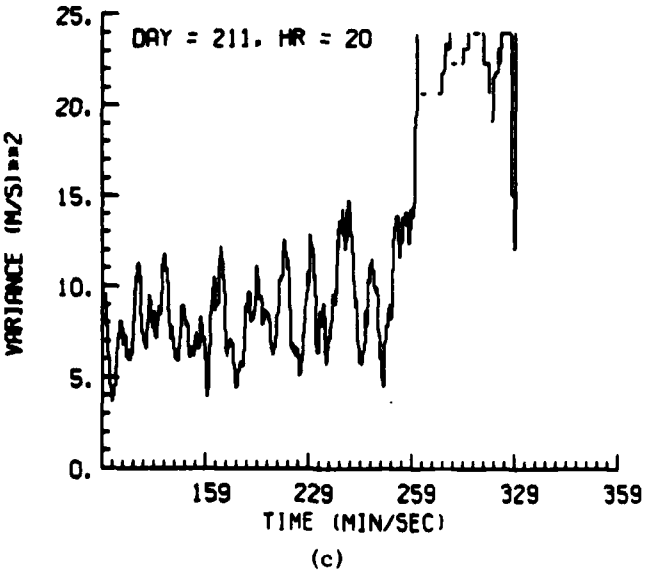

(c)

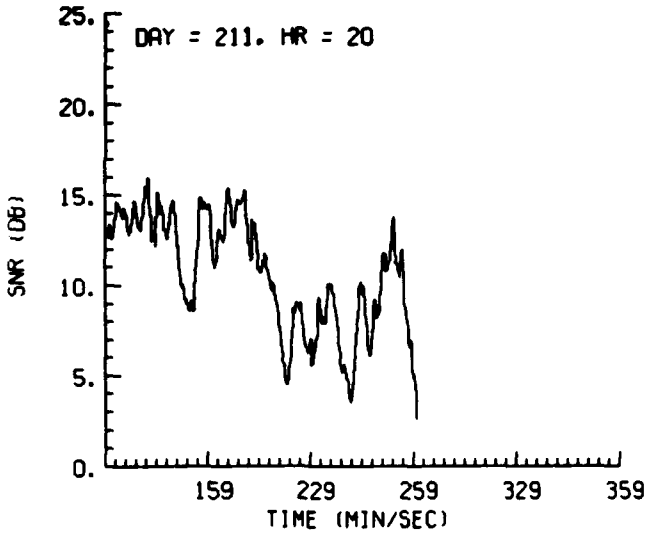

(d)

Figure A5. Time Histories of Doppler Spectrum Variance for: (a) Doppler, (b) Lob R-meter, (c) R-meter Estimators, and (d) Signal to Noise Ratio, for Penetration on 30 July 1982 (Contd)

Appendix B

Turbulence Severity Estimates

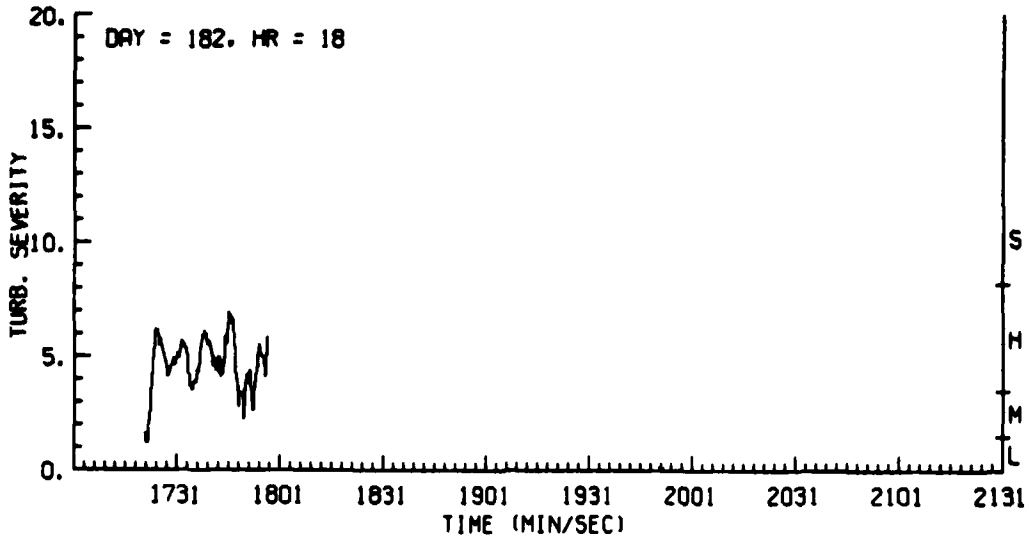

(a)

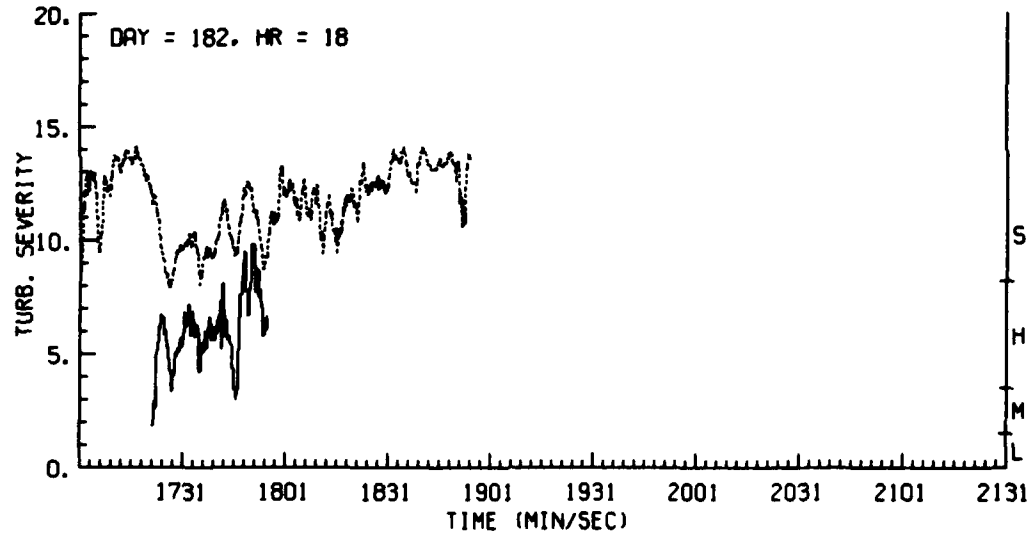

(b)

Figure B1. Time Histories of Turbulence Severity Derived From Doppler Spectrum Variance Estimates Using: (a) Doppler, and (b) Lob R-meter, and R-meter Estimators, for 1 July 1981

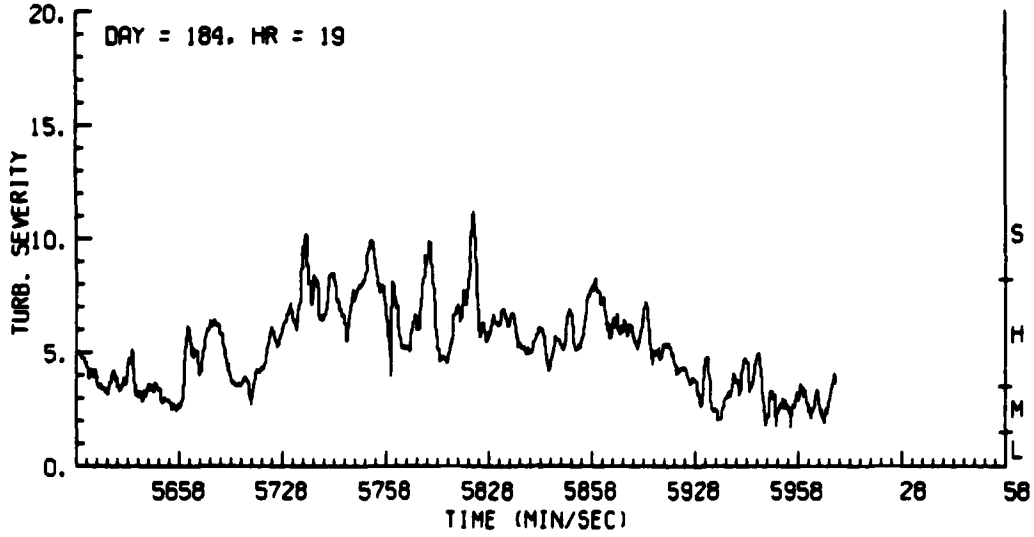

(a)

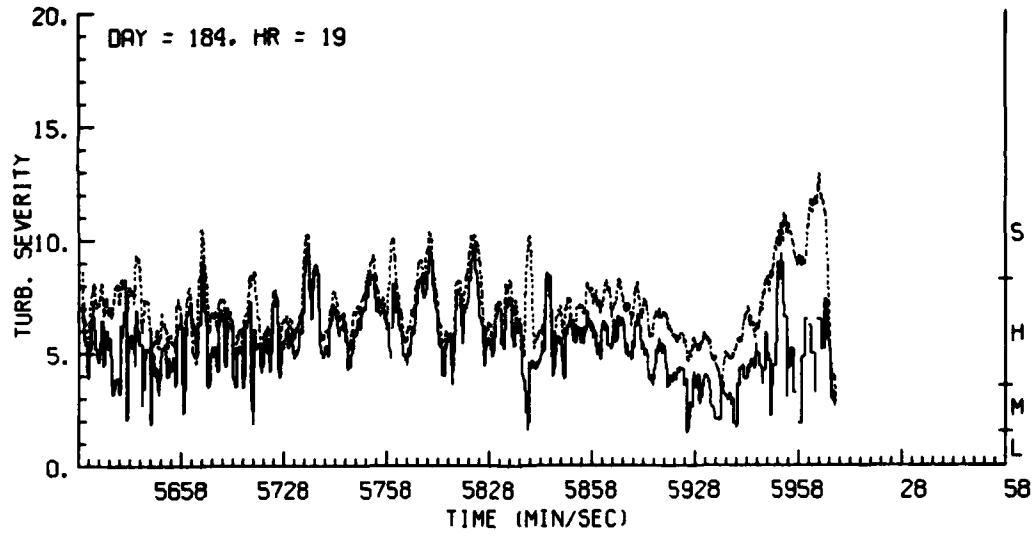

(b)

Figure B2. Time Histories of Turbulence Severity Derived From Doppler Spectrum Variance Estimates Using: (a) Doppler, and (b) Lob R-meter and R-meter Estimators for 3 July 1981

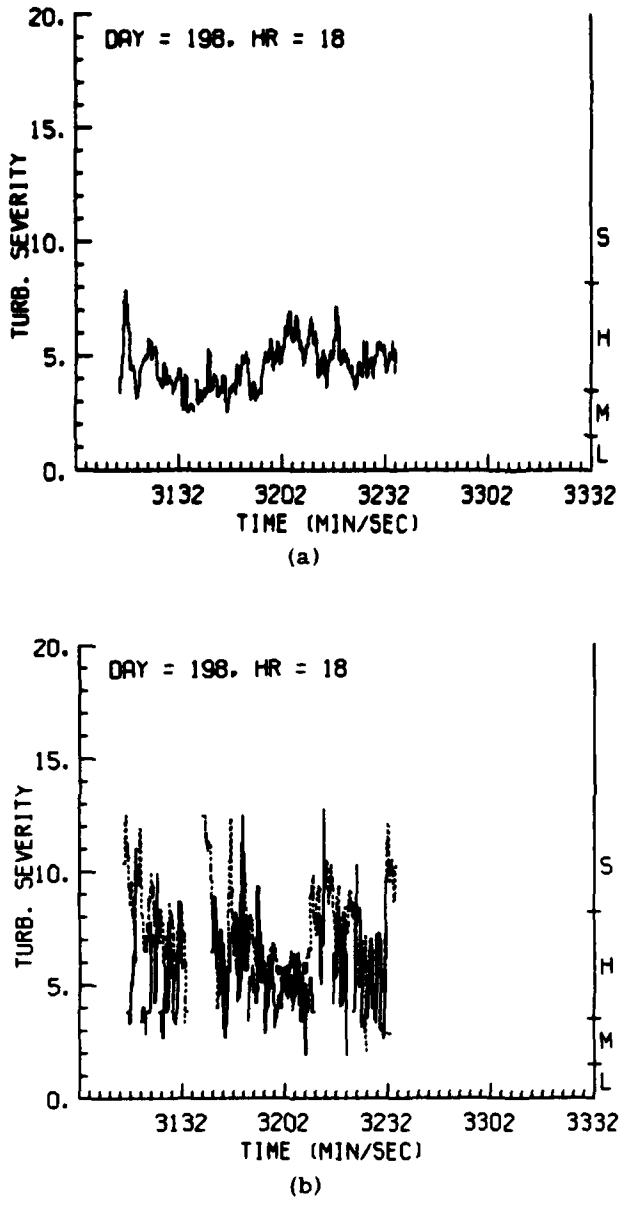

Figure B3. Time Histories of Turbulence Severity Derived From Doppler Spectrum Variance Estimates Using: (a) Doppler, and (b) Lob R-meter and R-meter Estimators, for 17 July 1981

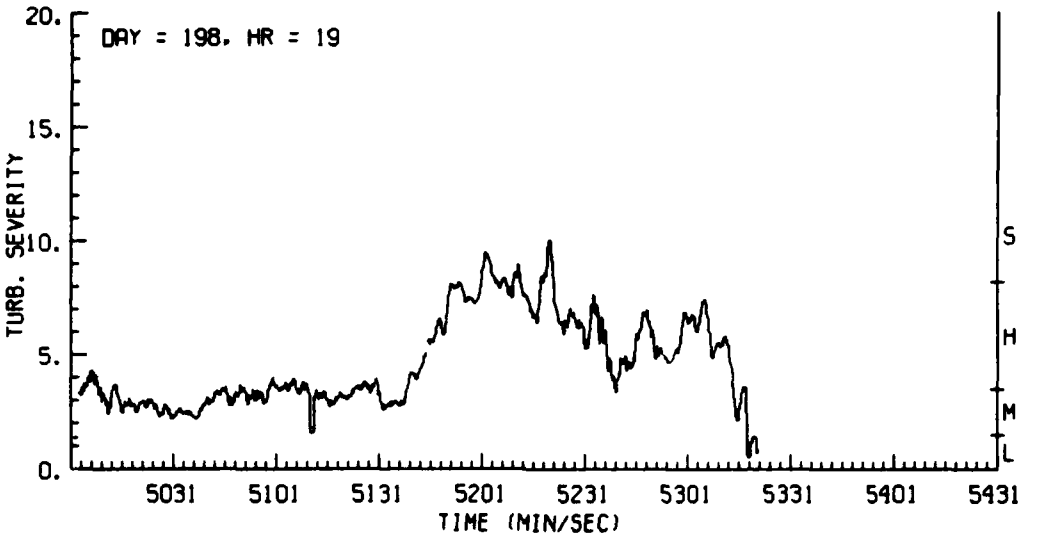

(a)

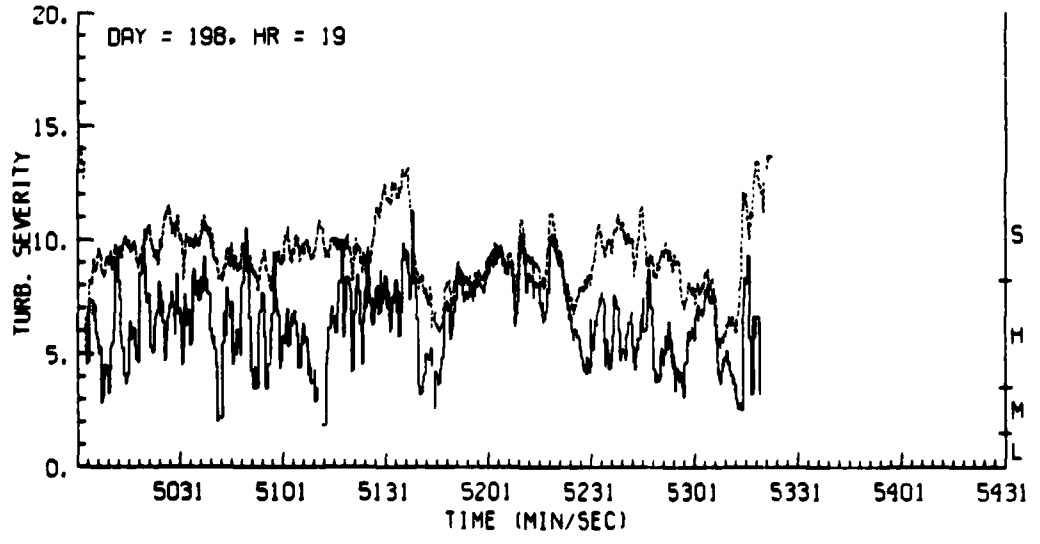

(b)

Figure B4. Time Histories of Turbulence Severity Derived From Doppler Spectrum Variance Estimates Using: (a) Doppler, and (b) Lob R-meter and R-meter Estimators, for 17 July 1982

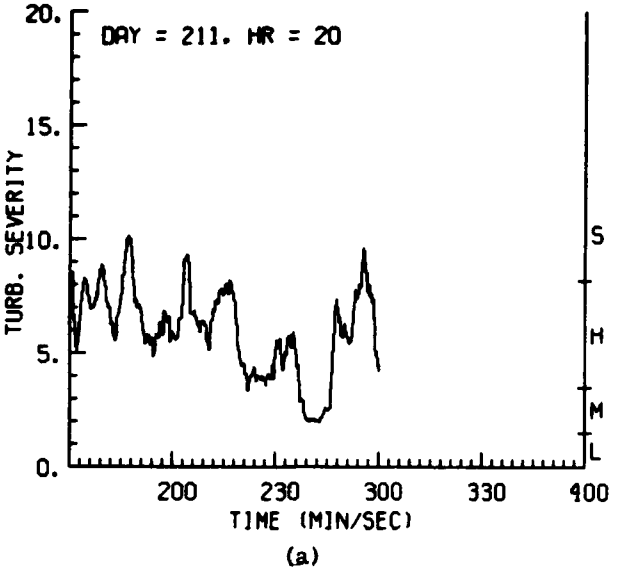

(a)

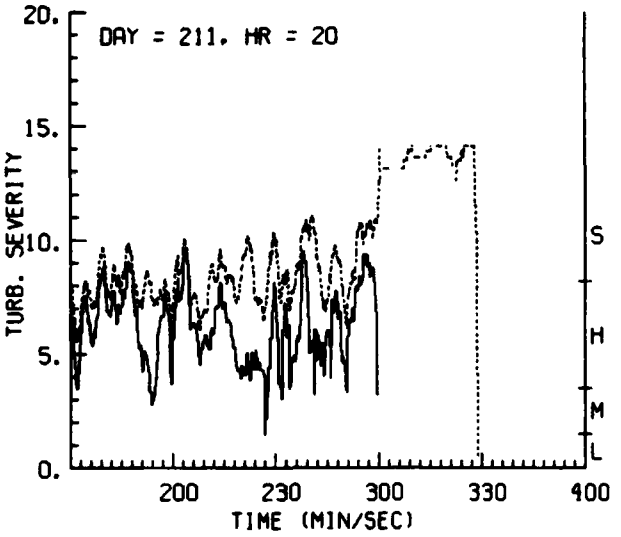

(b)

Figure B5. Time Histories of Turbulence Severity Derived From Doppler Spectrum Variance Estimates Using (a) Doppler, and (b) Lob R-meter and R-meter Estimators, for 30 July 1982

Appendix C

Aircraft Measurements of Turbulence Severity

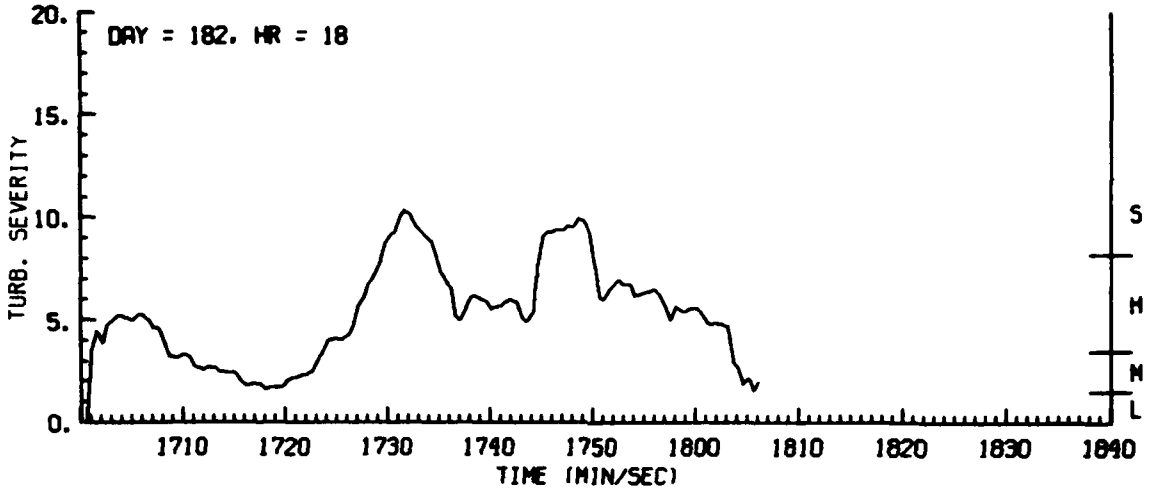

(a)

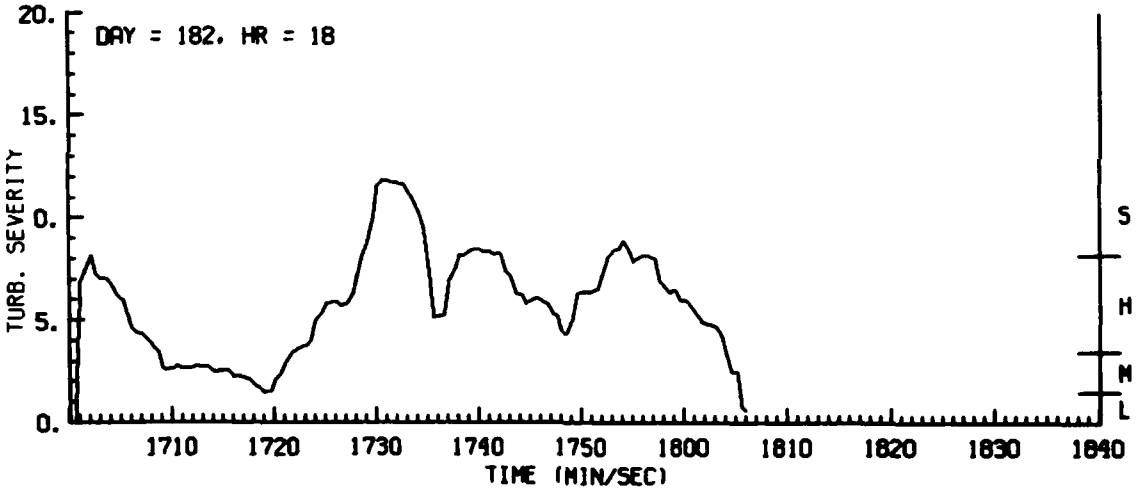

(b)

Figure C1. Time Histories of Turbulence Severity Derived From Aircraft Gust Data Along: (a) Longitudinal, (b) Lateral, and (c) Vertical Directions, for 1 July 1981

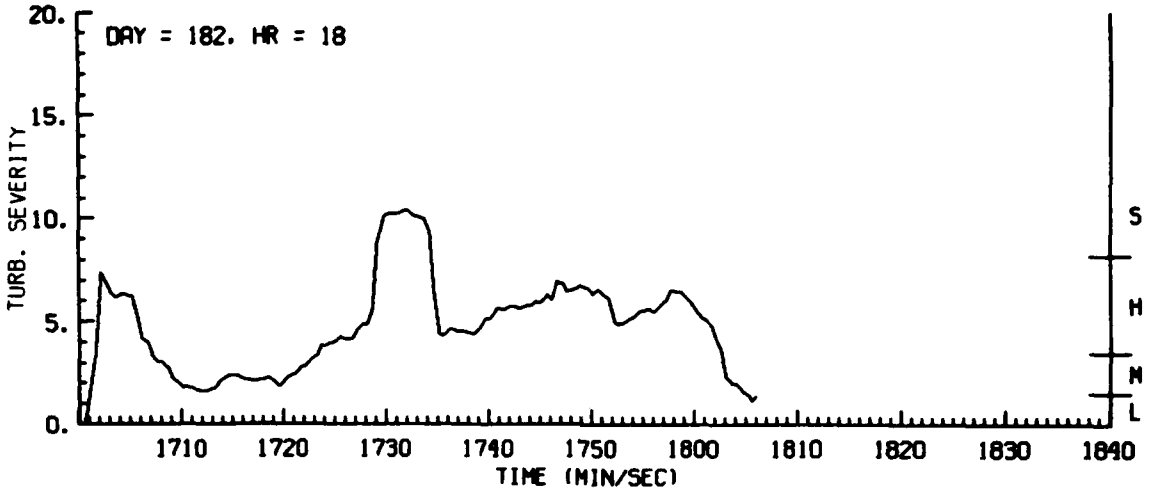

(c)

Figure C1. Time Histories of Turbulence Severity Derived From Aircraft Gust Data Along: (a) Longitudinal, (b) Lateral, and (c) Vertical Directions, for 1 July 1981 (Contd)

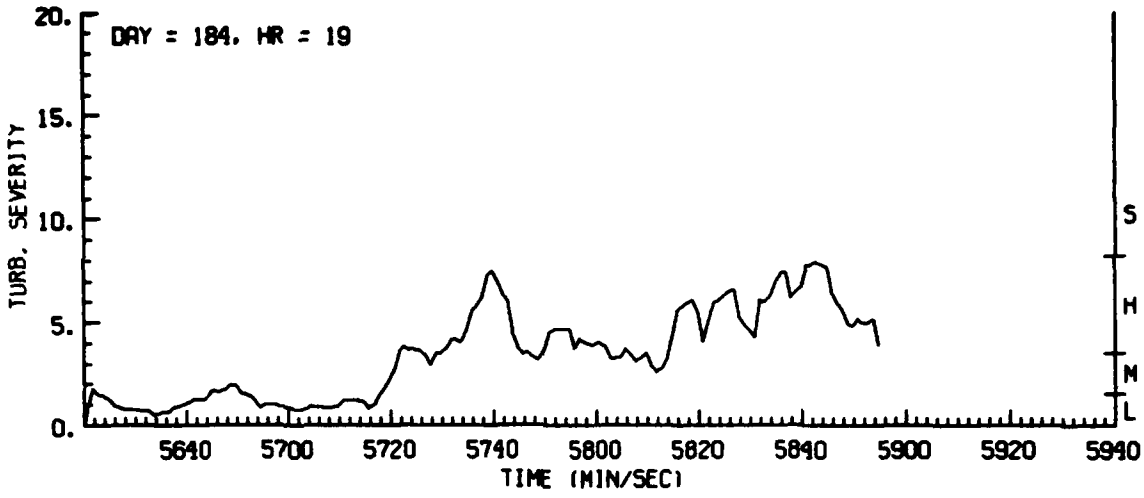

(a)

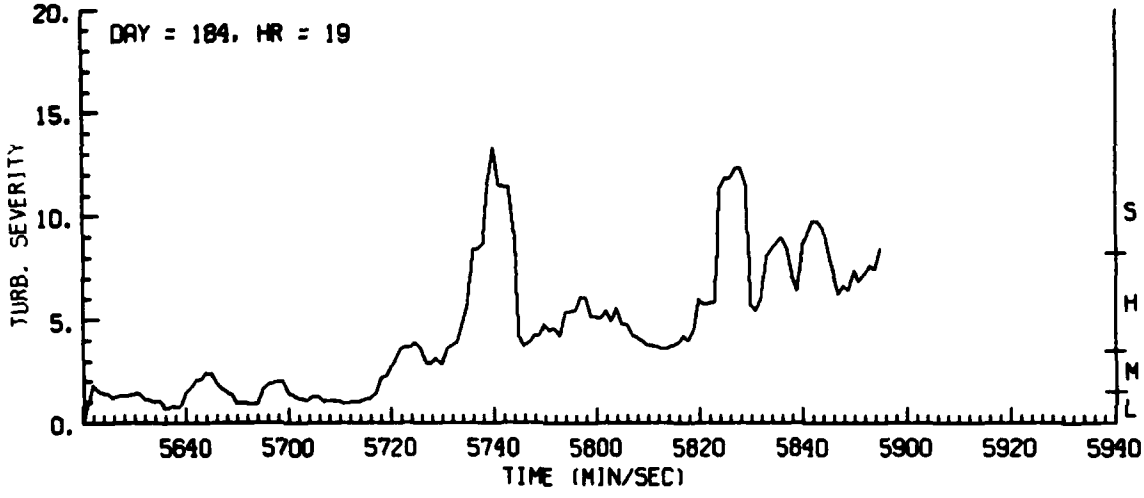

(b)

Figure C2. Time Histories of Turbulence Severity Derived From Aircraft Gust Data Along: (a) Longitudinal, (b) Lateral, and (c) Vertical Directions, for 3 July 1981

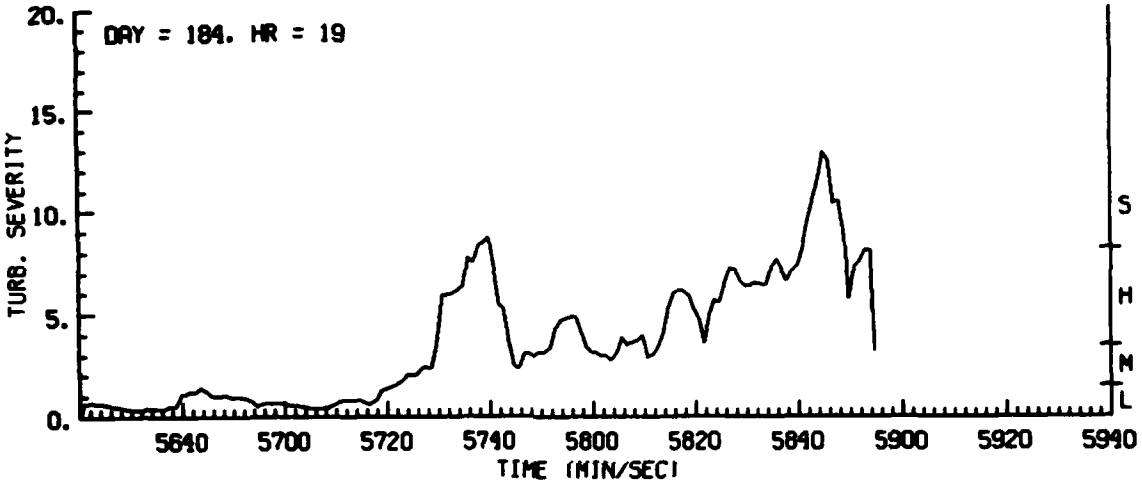

(c)

Figure C2. Time Histories of Turbulence Severity Derived From Aircraft Gust Data Along: (a) Longitudinal, (b) Lateral, and (c) Vertical Directions, for 3 July 1981 (Contd)

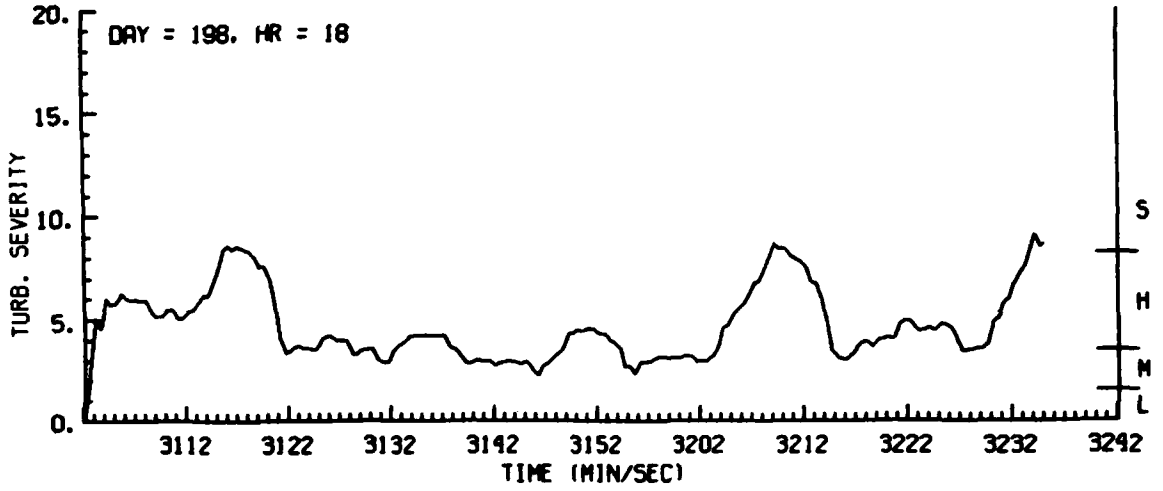

(a)

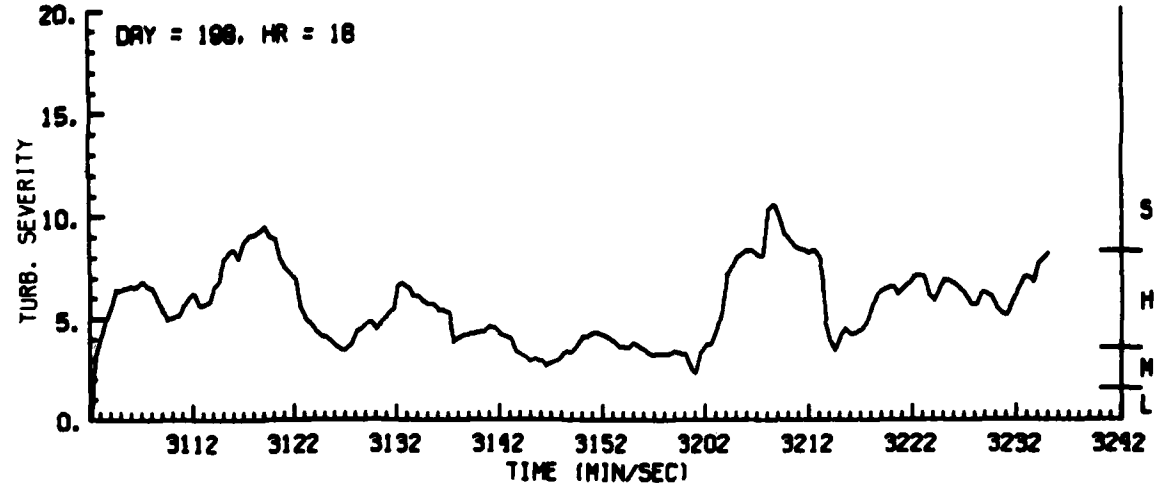

(b)

Figure C3. Time Histories of Turbulence Severity Derived From Aircraft Gust Data Along: (a) Longitudinal, (b) Lateral, and (c) Vertical Directions, for 17 July 1981

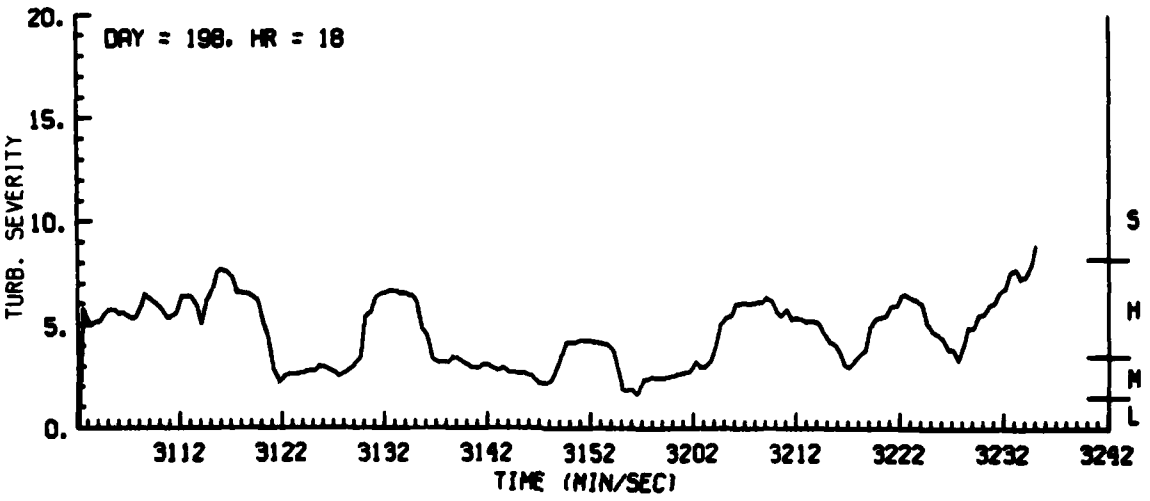

(c)

Figure C3. Time Histories of Turbulence Severity Derived From Aircraft Gust Data Along: (a) Longitudinal, (b) Lateral, and (c) Vertical Directions, for 17 July 1981 (Contd)

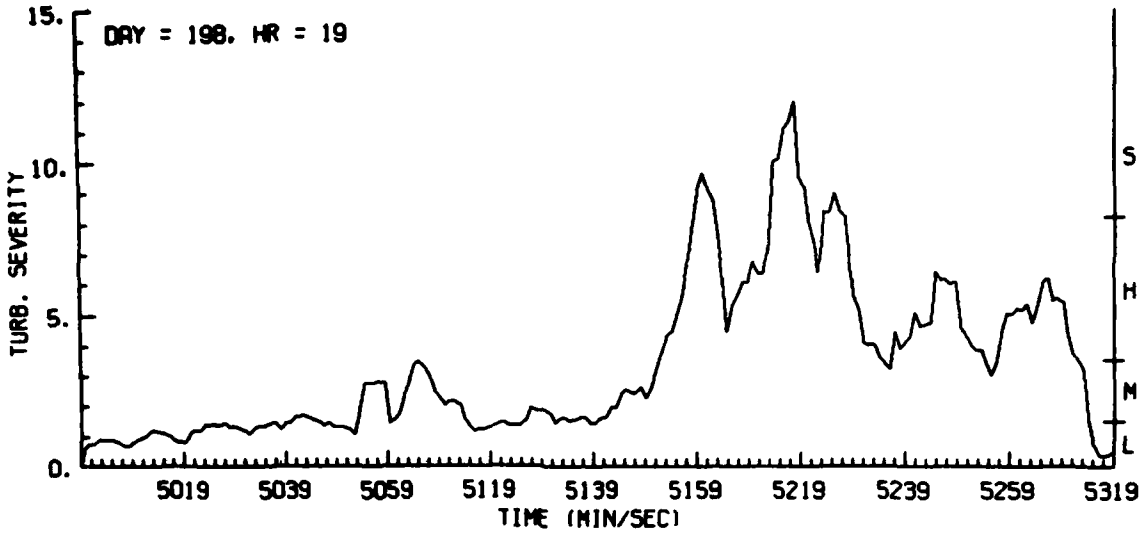

(a)

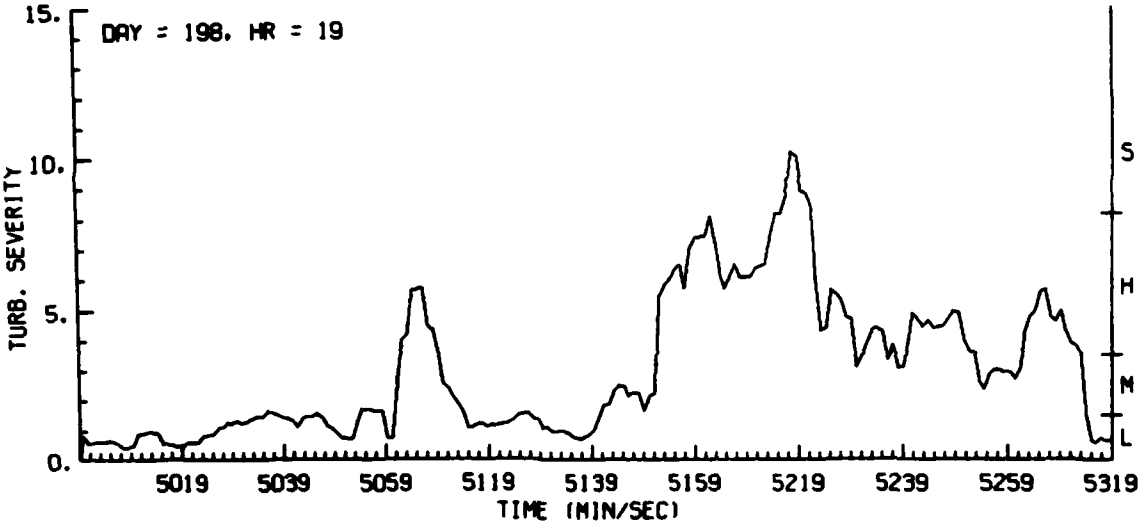

(b)

Figure C4. Time Histories of Turbulence Severity Derived From Aircraft Gust Data Along: (a) Longitudinal, (b) Lateral, and (c) Vertical Directions, for 17 July 1982

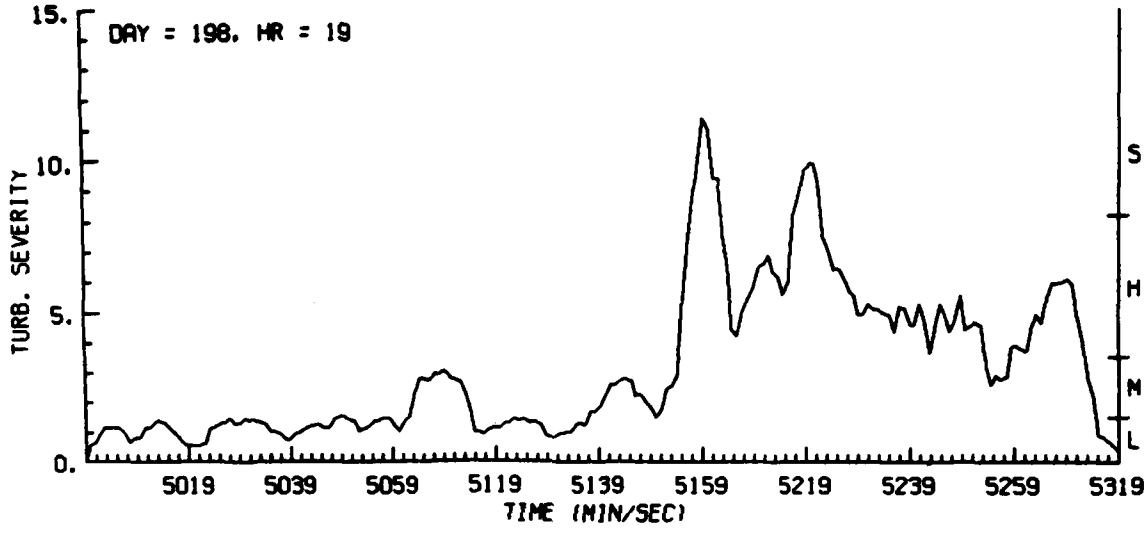

(c)

Figure C4. Time Histories of Turbulence Severity Derived From Aircraft Gust Data Along: (a) Longitudinal, (b) Lateral, and (c) Vertical Directions, for 17 July 1982 (Contd)

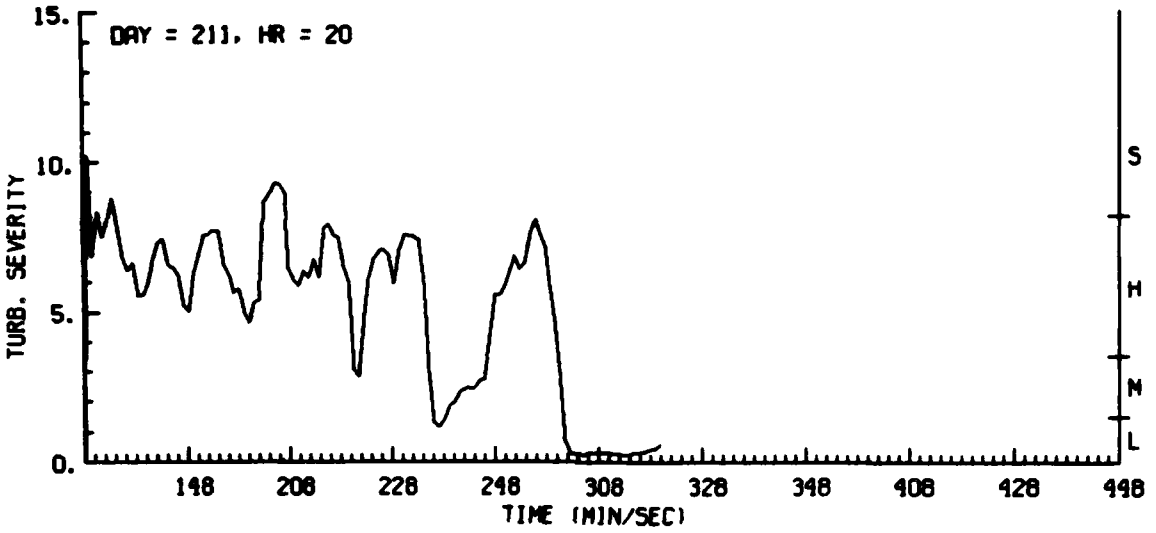

(a)

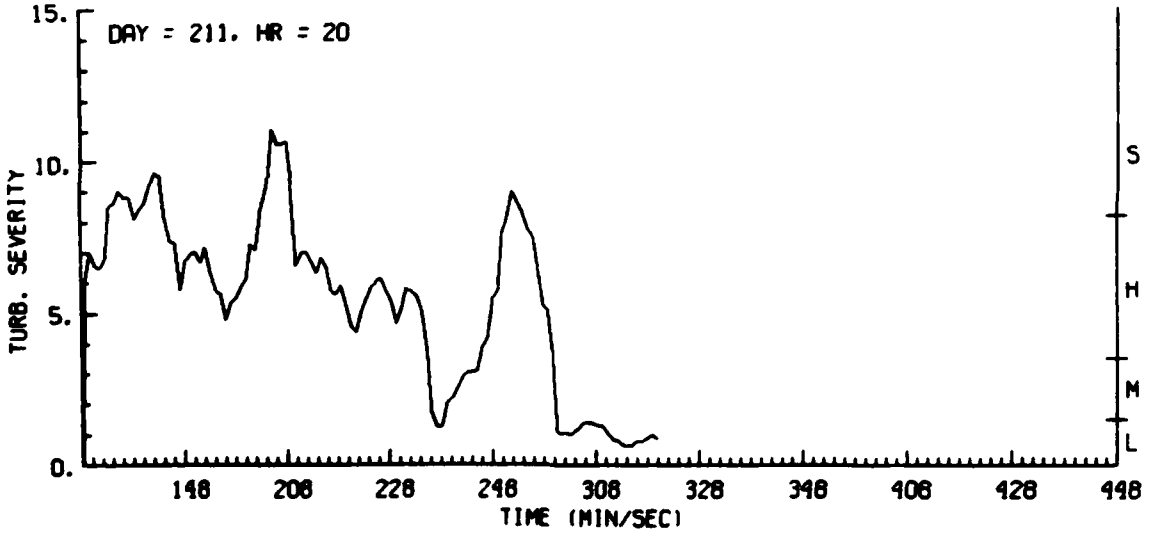

(b)

Figure C5. Time Histories of Turbulence Severity Derived From Aircraft Gust Data Along: (a) Longitudinal, (b) Lateral, and (c) Vertical Directions, for 30 July 1982

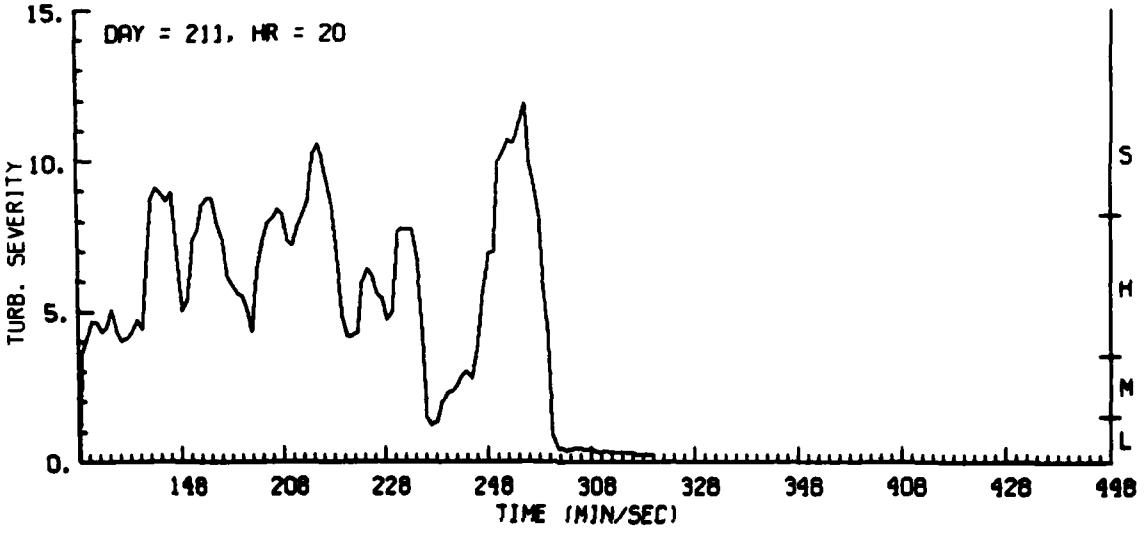

(c)

Figure C5. Time Histories of Turbulence Severity Derived From Aircraft Gust Data Along: (a) Longitudinal, (b) Lateral, and (c) Vertical Directions, for 30 July 1982 (Contd)

END

FILMED

11-85

DTIC